NAT'L INST. OF STAND & TECH
A11106 339821

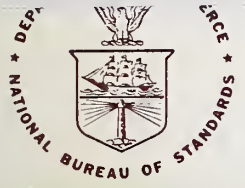

NBS TECHNICAL NOTE 1060

Reference
NBS
PUBLICATIONS

U.S. DEPARTMENT OF COMMERCE / National Bureau of Standards

Measurement of Multimode Optical Fiber Attenuation

QC
100
.U5753
No. 1060
1983

NATIONAL BUREAU OF STANDARDS

The National Bureau of Standards[1] was established by an act of Congress on March 3, 1901. The Bureau's overall goal is to strengthen and advance the Nation's science and technology and facilitate their effective application for public benefit. To this end, the Bureau conducts research and provides: (1) a basis for the Nation's physical measurement system, (2) scientific and technological services for industry and government, (3) a technical basis for equity in trade, and (4) technical services to promote public safety. The Bureau's technical work is performed by the National Measurement Laboratory, the National Engineering Laboratory, and the Institute for Computer Sciences and Technology.

THE NATIONAL MEASUREMENT LABORATORY provides the national system of physical and chemical and materials measurement; coordinates the system with measurement systems of other nations and furnishes essential services leading to accurate and uniform physical and chemical measurement throughout the Nation's scientific community, industry, and commerce; conducts materials research leading to improved methods of measurement, standards, and data on the properties of materials needed by industry, commerce, educational institutions, and Government; provides advisory and research services to other Government agencies; develops, produces, and distributes Standard Reference Materials; and provides calibration services. The Laboratory consists of the following centers:

Absolute Physical Quantities[2] — Radiation Research — Chemical Physics — Analytical Chemistry — Materials Science

THE NATIONAL ENGINEERING LABORATORY provides technology and technical services to the public and private sectors to address national needs and to solve national problems; conducts research in engineering and applied science in support of these efforts; builds and maintains competence in the necessary disciplines required to carry out this research and technical service; develops engineering data and measurement capabilities; provides engineering measurement traceability services; develops test methods and proposes engineering standards and code changes; develops and proposes new engineering practices; and develops and improves mechanisms to transfer results of its research to the ultimate user. The Laboratory consists of the following centers:

Applied Mathematics — Electronics and Electrical Engineering[2] — Manufacturing Engineering — Building Technology — Fire Research — Chemical Engineering[2]

THE INSTITUTE FOR COMPUTER SCIENCES AND TECHNOLOGY conducts research and provides scientific and technical services to aid Federal agencies in the selection, acquisition, application, and use of computer technology to improve effectiveness and economy in Government operations in accordance with Public Law 89-306 (40 U.S.C. 759), relevant Executive Orders, and other directives; carries out this mission by managing the Federal Information Processing Standards Program, developing Federal ADP standards guidelines, and managing Federal participation in ADP voluntary standardization activities; provides scientific and technological advisory services and assistance to Federal agencies; and provides the technical foundation for computer-related policies of the Federal Government. The Institute consists of the following centers:

Programming Science and Technology — Computer Systems Engineering.

[1]Headquarters and Laboratories at Gaithersburg, MD, unless otherwise noted; mailing address Washington, DC 20234.
[2]Some divisions within the center are located at Boulder, CO 80303.

NBS
RESEARCH INFORMATI
CENTER

NBS Technical Note 1060

QC
100
U5753
No.106
1983

Measurement of Multimode Optical Fiber Attenuation

R. L. Gallawa
G. E. Chamberlain
G. W. Day
D. L. Franzen
M. Young

Electromagnetic Technology Division
National Engineering Laboratory
National Bureau of Standards
Boulder, Colorado 80303

U.S. DEPARTMENT OF COMMERCE, Malcolm Baldrige, Secretary

NATIONAL BUREAU OF STANDARDS, Ernest Ambler, Director

June 1983

National Bureau of Standards Technical Note 1060
Nat. Bur. Stand. (U.S.), Tech. Note 1060, 52 pages (June 1983)
CODEN: NBTNAE

U.S. GOVERNMENT PRINTING OFFICE
WASHINGTON: 1983

For sale by the Superintendent of Documents, U.S. Government Printing Office, Washington, DC 20402
Price $4.00
(Add 25 percent for other than U.S. mailing)

CONTENTS

		Page
1.	Introduction	1
2.	Launch Conditions	5
	2.1 Phase Space	5
	2.1.1 A Summary of Phase Space Concepts	14
	2.2 LPS Launch	16
	2.3 Mode Filter Launch	18
3.	Component and System Variabilities	22
	3.1 Spot Size and Launch Numerical Aperture	22
	3.2 Mode Filter Qualification	28
	3.3 Component Linearity	31
	3.4 System Linearity	31
	3.5 System Noise	32
	3.6 Detector Uniformity	33
	3.7 Measurement Procedure	33
	3.8 Some Results	37
4.	Measurement Comparisons and Results	37
	4.1 Participants and Instructions	37
	4.2 Comparison Results	38
	4.3 Attenuation Measurements in High-DMA Fibers	41
	4.4 Summary of Interlaboratory Comparisons	43
5.	References	43
Appendix A.	Mode Volume and Limited Phase Space	45

Measurement of Multimode Optical Fiber Attenuation

R. L. Gallawa, G. E. Chamberlain, G. W. Day,
D. L. Franzen, and M. Young*

National Bureau of Standards
Boulder, Colorado 80303

This document is one of a series which describes optical fiber measurement capabilities at the National Bureau of Standards. We concentrate here on the measurement of attenuation of multimode, telecommunication-grade fibers for the wavelength range of 850 nm to 1300 nm. The document begins by discussing the need for restricted launch conditions, the most fundamental and crucial aspect of precise attenuation measurements. The limited phase space launch (also called the beam optics launch) and the mode filter launch are discussed. Attention then turns to the practical matter of ensuring that the conditions of the restricted launch are met. Discussions of system noise and system linearity are also included. The document describes measurement procedure and results obtained in the laboratory using three typical fibers. Results are presented for the two wavelengths of current interest: 850 nm and 1300 nm. The procedures are applicable to any wavelength, however. The document touches briefly on the matter of monomode fibers. Finally, a summary of the results from an interlaboratory comparison are presented to give perspective to the stability of a fiber subjected to handling and shipping.

Key words: attenuation; attenuation measurement; fiber measurement; optical fibers; optical waveguides.

1. Introduction

Two operational parameters are basic to the utility of any transmission line: attenuation and bandwidth. These two determine repeater spacing and ultimate cost of a telecommunication network. Both must be characterized because either attenuation or bandwidth may limit the range-bandwidth product of a communication link; the range-bandwidth product is the most frequently used measure of performance and cost. Full exploitation of system components depends on an understanding of which parameter (bandwidth or attenuation) is restricting system capability.

The techniques described in this document are applicable to all wavelengths of interest for telecommunications. The measurements reported on, however, were done at only 850 nm and 1300 nm. The system uses an incandescent strip filament light source in conjunction with interference filters for wavelength selection. Thus, it is amenable to measurement at discrete wavelengths.

We restrict attention to telecommunications-quality graded-index multimode fibers. Such fibers have a nominally 50 μm core diameter and the refractive index profile is carefully controlled. Usually the profile is nearly parabolic, yielding high bandwidth. The loss in telecommunication-grade fibers is as low as practical. Fibers used in short-distance applications or LAN (local area networks) are frequently large core fibers and often have a step index profile. The attenuation is less important than it is for long haul fibers. Even if the fibers used in the two applications (long and short distances) were identical, the philosophy behind the measurement technique would undoubtedly

*Electromagnetic Technology Division, National Engineering Laboratory.

be different in the two cases. For long distance fibers, the measured value of attenuation should be indicative of the attenuation experienced in a long link. Likewise, the attenuation measured for a short distance fiber should be representative of the attenuation experienced in a typical short distance application. The modal power distribution at launch is important to the measured value of attenuation in each case.

The philosophy of improving measurement precision by restricting the launch is intimately related to the excitation of high-loss modes, including leaky modes. The concept is distinctly different in graded-index and step-index fibers. By uniformly illuminating the fiber core using a limited launch numerical aperture, one avoids the excitation of high-order and leaky modes of a step-index fiber. This is not true when the fiber has a graded refractive index because the local numerical aperture of the fiber is a function of radial position.

A launch condition that works well for step-index fibers may not work well for graded-index ones. The converse is also true: a launch condition that yields usable results for a graded-index fiber may not be the most suitable one for step-index fibers. The reported attenuation must be meaningful in the context of its application. Short-haul links using LED sources are not considered in this document. We are concerned here with the characterization of fibers in a way that will be useful in predicting the performance of a telecommunication link, which may include concatenated fibers.

Monomode fibers, though not considered in this document, are important in high capacity, long haul systems, where attenuation is more likely to be the limiting parameter in system design. Launch conditions are simpler for monomode fibers since only the fundamental mode will propagate. A mode filter or limited launch numerical aperture is therefore not necessary. The fiber will support two orthogonal polarization states and this may be a source of inaccuracy if the light is polarized. Coupling between the polarization states of the fiber may be difficult to control. Furthermore, the attenuation coefficient is different for the two states. The problems associated with the birefringence of the fiber are especially important in systems that are phase sensitive. A meaningful characterization of the monomode fiber is difficult in that case.

Fiber attenuation is the diminution of average optical power, measured in decibels. The rate of diminution, with respect to distance, is known as the attenuation coefficient for the fiber, usually denoted by α, and is specified in decibels/kilometer. If α is constant, the attenuation of a length L of fiber is

$$\alpha L(\mathrm{dB}) = -10 \log [P(L)/P(0)], \tag{1-1}$$

where P(L) is the power at distance L from the reference position where the power is P(0) and log indicates the common logarithm. In practice, the attenuation coefficient varies with distance and operating wavelength, λ. The parameter of interest, then, is the average attenuation of the fiber, as found from eq (1-1), where

$$\frac{P(L,\lambda)}{P(0,\lambda)} = 10^{-\int_0^L \frac{\alpha(z,\lambda)dz}{10}}. \tag{1-2}$$

The obvious method of measuring attenuation, then, is as follows: power reaching a detector through two different lengths of fiber (L_0, L_1) is measured for the operating wavelength of interest. The average attenuation coefficient is

$$\alpha(\lambda) = \frac{10}{L_1 - L_0} \log \frac{P(L_0)}{P(L_1)} . \qquad (1\text{-}3)$$

In this form, attenuation is positive if $L_1 > L_0$.

For graded-index multimode fibers, the utility of such a measurement depends on how power was launched into the fiber. The transmitted power resides in a finite number of modes, and different modes have different attenuation coefficients. Thus, the measured average attenuation of a multimode fiber depends on the relative amount of power in each mode. At launch, the relative power depends on launch conditions. A small LD (laser diode) may launch its power into the center region of the fiber but overfill the fiber numerical aperture. An LED (light-emitting diode) has a broad angular radiation pattern and large size so it excites all modes more or less uniformly. Clearly, the attenuation measured using an LED source is different from that measured using an LD. This difference in attenuation disappears after the fiber reaches the steady-state or condition of equilibrium modal power distribution, in which case the relative power in the various modes is independent of length. Thus, the modal power distribution at the output is independent of the modal power distribution at input. The equilibrium condition is achieved beyond a certain propagation distance called the equilibrium length. The condition is reached after the high-loss modes have been attenuated or coupled into modes which have less attenuation. In the steady-state condition, intermodal coupling is in equilibrium, so power coupled from one mode to the others is just compensated by differential attenuation and power coupled in the opposite direction. The effect of an equilibrium modal power distribution is shown in figure 1-1 (after ref. 1) which shows the result of length-dependent measurements on a 4 km length of parabolic profile fiber at 800 nm and 1060 nm. The launch numerical aperture is 0.10 in each case. Steady state appears to be reached after about 2 km. For shorter lengths, the attenuation coefficient is higher than the steady-state value; this can be attributed to the presence of high-loss modes. The slope of the curve at any point gives the local attenuation coefficient. The slope (attenuation coefficient) in the first kilometer of fiber is significantly higher than in the fourth kilometer of the same fiber. This figure illustrates, then, the need for launch conditions which create the desired power distribution and, hence, lead to attenuation values that are typical of long fibers.

More recent results show a similar trend but the distance required to reach steady state is considerably reduced [2]. Recent data confirm that differential mode attenuation is considerably less today than it was just a few years ago. Furthermore, differential mode attenuation is a function of operating wavelength, so the distance required to reach steady state changes with a change in operating wavelength.

The two launch conditions used in this report are the LPS (limited phase space) launch (also called the beam optics launch) and the mode filter launch. In the first, the launch spot size and the launch numerical aperture are adjusted to be, respectively, 70 percent of the fiber core size and 70 percent of the fiber numerical aperture. The condition is therefore also referred to as the 70/70 launch condition. The LPS launch apparatus is more complicated than the mode filter launch because the apparatus must allow for independent adjustment of launch spot size and launch angle. The product of launch spot size and launch angle is related to phase space volume, discussed in section 2.1.

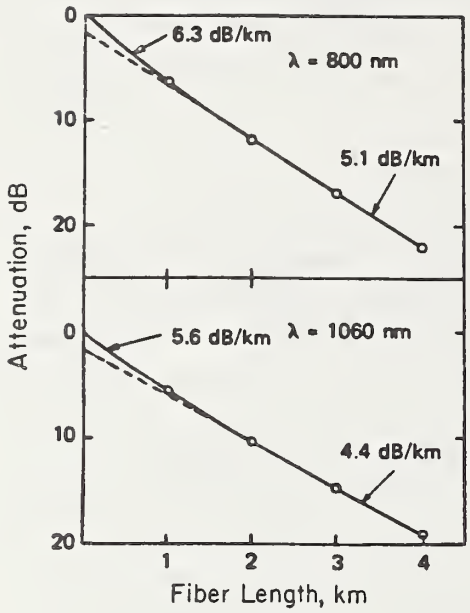

Figure 1-1. Loss in a 4 km length of parabolic profile fiber. Launch NA = 0.1 in each case. After reference 1.

The mode filter launch calls for launch spot size and launch angle larger than fiber core size and fiber numerical aperture. The launch optics can therefore be rather simple. The overfilled fiber is subjected to a filter, the purpose of which is to establish a modal power distribution that approximates the modal power distribution at the end of a long fiber without the filter. The mode filter is deemed appropriate if a short length of the test fiber which is subjected to the filter produces a far-field radiation pattern that is similar (within tolerance) to that of the long test fiber without the filter.

Details on the two launch conditions are given in section 2.

The problems discussed here are not applicable to monomode fibers, where the optical size of the fiber is so small that only a single mode can propagate.

Since the strength of intermodal coupling influences the attenuation of the fiber, the environment can affect the measured attenuation. The loss value assigned to an uncabled fiber may not be appropriate to the cabled fiber. Likewise, the loss of an uncabled fiber on a spool depends on how tightly the fiber is wrapped around the spool.

For purposes of fiber specification (i.e., for purposes of trade and commerce) it is important that the attenuation assigned to a fiber be of practical use. When fibers are concatenated, the attenuation of the resulting link should be predictable from the specified attenuation of individual fiber sections. That is the crux of the attenuation measurement problem.

In this report, we discuss specific details of a meaningful measurement technique. Before proceeding, however, we note that the mode coupling discussed above has a beneficial effect on fiber bandwidth as well. Different modes have different phase and group velocities, as well as different attenuations. The duration of a pulse increases as it propagates in a multimode fiber. The increased duration results from different group velocities of the different modes. Initially, pulse duration usually increases linearly with distance, but for lengths exceeding the equilibrium length, the pulse duration may increase more slowly with distance, approaching $L^{1/2}$ variation in some cases [3,4].

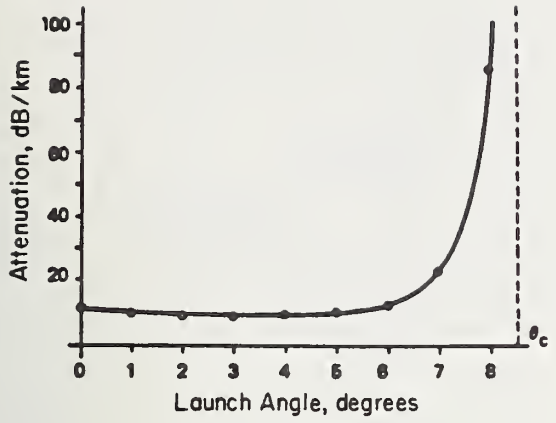

Figure 2-1. Attenuation coefficient as a function of input plane wave angle at 632.8 nm (after ref. 5).

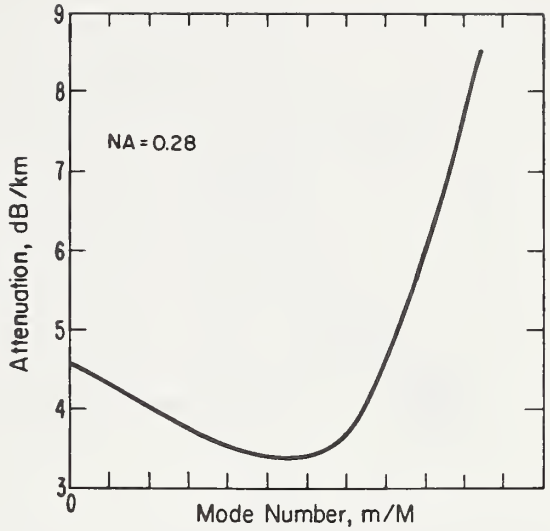

Figure 2-2. Symbolic representation of 0.28 NA fiber waveguide attenuation at 800 nm as a function of mode number. Mode number was altered by changing launch spot position but not launch angle. Launch angle is 0 (after ref. 6).

2. Launch Conditions

That different modes have different attenuation coefficients is intuitive. Figures 2-1 and 2-2 [5,6] give experimental evidence to support the allegation. Figure 2-1 shows the attenuation coefficient as a function of input launch angle for a step-index fiber at 6328 nm. The high-order modes associated with the steep input angles show a very high attenuation per unit length. In contrast, the low-order rays have fairly uniform attenuation. Clearly then, the input launch condition plays an important role in the measured attenuation. Figure 2-2 is symbolic of the attenuation coefficient as a function of normalized mode number at 800 nm for a graded fiber having 0.28 NA. Both scattering and absorptive loss have been accounted for in this curve [6]. In the figure, M is the mode volume of the fiber or the total number of modes the fiber will support (cf. appendix A). m is the counting index that identifies the mode number.

A complete description of modal properties and how those properties influence fiber attenuation is beyond the scope of this manuscript. The reader is referred to the references for additional details [7]. For our purposes, we concentrate on the launch conditions and how those conditions influence the excitation of various modes. To that end, we digress briefly to discuss the concept of phase space. That concept is fundamental to one of the two launch conditions discussed in this document. Those conditions are discussed later in this section.

2.1 Phase Space

The concept of phase space is basic to the limited phase space launch condition. In this section, we give some basic definitions and connecting relationships that lend credence to the proposition that the LPS launch is a reasonable one to use. The reader who is not interested in these connecting relationships can skip directly to section 2.2 or he may pause to read the summary paragraphs in section 2.1.1.

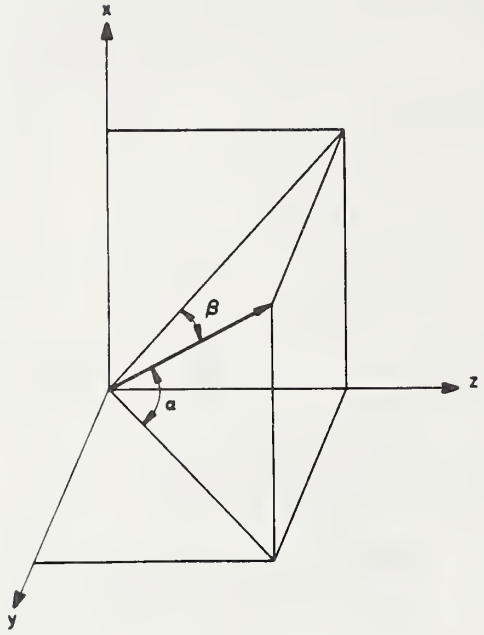

Figure 2-3. A typical light ray and angles in a rectangular coordinate system.

Phase space and its relationship to the problem of coupling optical energy to and from a source is understood by noting first that a light ray has "momentum" which depends on its position and direction. If the optical axis is the z-axis of a rectangular (x,y,z) coordinate system, the momentum of the ray depends on x, y, dx/ds and dy/ds, where x,y is its location and ds is its incremental distance along the ray path. In particular, the momenta in the x and y directions are

$$p_x = n\, dx/ds, \tag{2-1a}$$

$$p_y = n\, dy/ds, \tag{2-1b}$$

where n is the refractive index at x, y and may be a function of position. Figure 2-3 shows a typical light ray and its angle with respect to the axial (z) direction. In this case,

$$p_x = n \sin \alpha, \tag{2-2a}$$

$$p_y = n \sin \beta. \tag{2-2b}$$

The physical state of a ray is completely specified by the four variables x, y, p_x, p_y. These four variables define a four-dimensional space called the phase space. The position of a ray in phase space has a one-to-one relationship with its trajectory in physical space.

The power coupled into a fiber mode depends on the trajectory of the launch ray so it is not surprising that these concepts should be encountered in a discussion of restricted launch conditions. Indeed, the efficiency of coupling between fibers or between a fiber and a terminal device (e.g., a light source) is characterized by the phase space match. The conservation of radiance, for example, is a manifestation of this concept, as will be seen below. For the purpose of measuring fiber attenuation, we seek to establish a launch condition for which the phase space matches the phase space desired in the fiber.

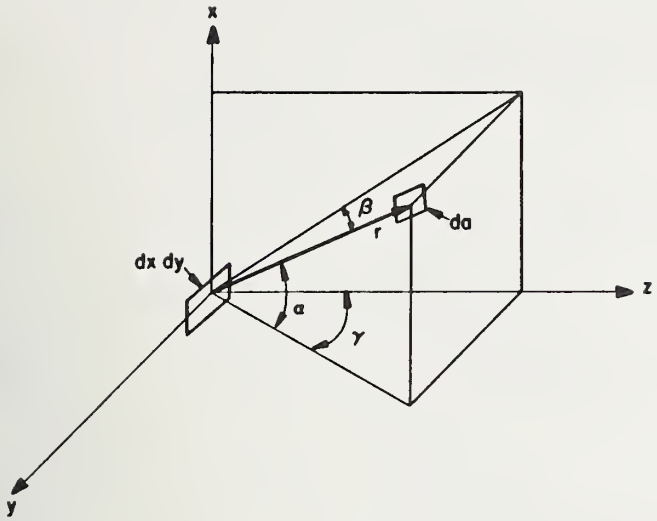

Figure 2-4. Illustrating angles and areas used to discuss phase space.

Optical coupling depends on the density of points in phase space. Each ray in a bundle of rays is represented by a point in phase space, and the collection of rays in the bundle corresponds to a volume (denoted ψ) in phase space. As the ray bundle moves through physical space, the direction and location of the rays change; this corresponds to a change in location of the various points in phase space. The density of points ρ is the number of points per phase space volume. One form of Liouville's theorem [8] demands that neither the density of points in phase space nor the phase space volume can change with axial direction; i.e., $d\rho/dz = 0$, $d\psi/dz = 0$.

Normally, and not unexpectedly, the density is defined in terms of the incremental power, dP, in an increment of phase space volume $d\psi$.

$$\rho = dP/d\psi. \tag{2-3}$$

This equation shows that radiance is proportional to density, as will be seen. The total power (or, equivalently, the total number of rays) is found by integrating over phase space:

$$P = \int dP = \int \rho d\psi = \int \rho \, dxdydp_x dp_y. \tag{2-4}$$

Figure 2-4 shows the relationship between the differential volume element in phase space and the product of differential area and differential solid angle in physical space. The area dxdy is normal to the z-axis and could represent a source radiating into the right-half plane. The figure shows that

$$p_x = n \sin \alpha, \tag{2-5a}$$

$$p_y = n \cos \alpha \sin \gamma = n \sin \beta, \tag{2-5b}$$

$$dp_x = n \cos \alpha \, d\alpha, \tag{2-5c}$$

$$dp_y = n \cos \alpha \cos \gamma \, d\gamma = n \cos \beta \, d\beta. \tag{2-5d}$$

The differential volume in the plane $z = 0$ is

$$d\psi = dxdy\ n^2 \cos^2 \alpha \cos\gamma\ d\alpha\ d\gamma. \tag{2-6}$$

The projection of the source normal to the ray is

$$da = dxdy \cos\alpha \cos\gamma = rd\alpha\ r \cos \alpha\ d\gamma. \tag{2-7}$$

The solid angle encompassed by da is therefore

$$d\Omega = da/r^2 = \cos \alpha\ d\alpha d\gamma. \tag{2-8}$$

Thus,

$$d\psi = n^2\ dxdy\ d\Omega \cos\alpha \cos\gamma = n^2\ da\ d\Omega, \tag{2-9}$$

where da is normal to the ray.

This important connecting relationship between phase space and the product of area and solid angle is fundamental to one of the launch conditions used to measure attenuation. The relationship is a manifestation of the conservation of radiance, since

$$\rho = \frac{dP}{d\psi} = \frac{dP}{n^2 da\ d\Omega} = \frac{L}{n^2}\ , \tag{2-10}$$

where radiance L is, by definition,

$$L = \frac{dP}{da\ d\Omega}. \tag{2-11}$$

The requirement $d\rho/dz = 0$ is equivalent, then, to the conservation of radiance:

$$\frac{d}{dz}\left(\frac{L}{n^2}\right) = 0. \tag{2-12}$$

The concept of a LPS (limited-phase space) launch is based on eq (2-9) and the requirement that only bound modes having "reasonable" loss values should be launched when measuring attenuation. This leads to measured values that are reproducible (precise) and more or less independent of the person who made the measurement. The LPS launch calls for a launch spot size equal to 70 percent (actually, $\sqrt{0.5}$) of the fiber core diameter and a launch numerical aperture equal to 70 percent (actually, $\sqrt{0.5}$) of the fiber numerical aperture [9]. The reason for this selection is related to the power-accepting properties of a fiber and the concept of fiber NA (numerical aperture). To examine the relationship between fiber NA and phase space, consider the following.

The concept of fiber NA becomes slightly complex when leaky rays are considered [10]. A leaky ray (or, correspondingly, a leaky mode) is one for which geometric optics would predict total internal reflection at the core-cladding boundary, but which suffers loss by virtue of the curved core boundary. Specifically, a leaky ray is a ray located at radial position r and having direction such that

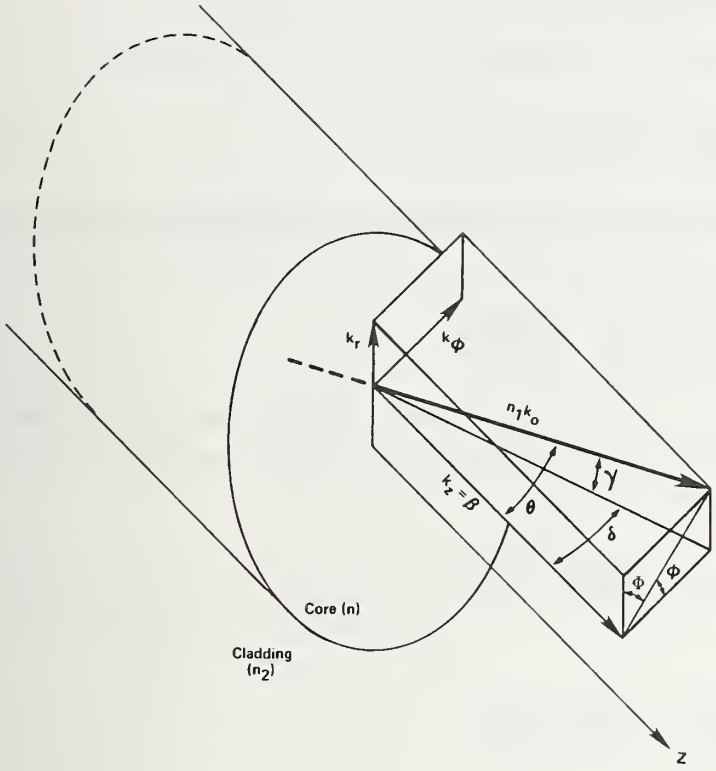

Figure 2-5. A typical light ray and angles in a fiber.

$$n^2(r) - n^2(a) \leq \sin^2 \theta(r) \leq \frac{n^2(r) - n^2(a)}{1 - (r/a)^2 \cos^2\phi(r)}, \tag{2-13a}$$

where $\theta(r)$ is the angle the ray makes with the waveguide axis, $n(r)$ is the r-dependent refractive index, a is the core radius, and $\phi(r)$ is the azimuthal angle of the projection of the ray on the transverse plane [11]. A bound ray is one for which

$$0 \leq \sin^2(\theta) \leq n^2(r) - n^2(a). \tag{2-13b}$$

Figure 2-5 shows a ray in a fiber; the angles appearing in eq (2-13) are shown, as are other angles, as well as the radial, azimuthal, and axial components of the wave vector k (k_r, k_ϕ, $k_z = \beta$); k_0 is the wave number in free space. Skew rays correspond to $\phi < \pi/2$; meridional rays correspond to $\phi = \pi/2$. Meridional rays always traverse the fiber axis while skew rays never do.

If leaky rays are included, the local numerical aperture of a fiber (which determines whether or not an incident ray is accepted) is defined as

$$NA = (NA)_o \left[\frac{1 - (r/a)^g}{1 - (r/a)^2 \cos^2\phi}\right]^{1/2} \tag{2-14}$$

where

$$(NA)_o = (n_1^2 - n_2^2)^{1/2} \tag{2-15}$$

and g is the power-law profile parameter; i.e., it is assumed that

$$n(r) = n_1[1 - 2\Delta(r/a)^g]^{1/2}, \tag{2-16}$$

where n_1 is the refractive index at r = 0; Δ is the contrast, specifying the difference between n(0) and $n(a) = n_2$. If $\phi = \pi/2$,

$$NA]_{\phi=\pi/2} = (NA)_o[1 - (r/a)^g]^{1/2}. \tag{2-17}$$

The power accepted by the fiber at any point on the core is proportional to the square of the numerical aperture. The equation for $(NA)^2$ is the equation of an ellipse, which degenerates to a circle at r = 0. The ellipse has semi-major axis

$$(NA)_o \left[\frac{1 - (r/a)^g}{1 - (r/a)^2}\right]^{1/2}, \tag{2-18}$$

and semi-minor axis

$$(NA)_o[1 - (r/a)^g]^{1/2}. \tag{2-19}$$

The area of the ellipse is proportional to the product of these two axes:

$$\text{Area} = \pi(NA)_o^2 \frac{1 - (r/a)^g}{[1 - (r/a)^2]^{1/2}}. \tag{2-20}$$

At r = 0, the circle that describes NA has area $\pi(NA)_o^2$. The ratio of the two areas is the ratio of power accepted by the fiber at radius r to that accepted at r = 0:

$$\frac{P(r)}{P(0)} = \frac{1 - (r/a)^g}{[1 - (r/a)^2]^{1/2}}. \tag{2-21}$$

This result can also be obtained from the phase space representation using the notation of figure 2-5. For the circular cylindrical system

$$d\psi = dA \sin\theta \cos\theta \, d\theta \, d\phi, \tag{2-22a}$$

where dA is the incremental area on the fiber core. The fiber near field, as given in eq (2-21), is obtained by integrating $d\psi/dA$ over all angles:

$$\frac{P(r)}{P(0)} = \frac{\int_0^{\pi/2} d\phi \int_0^{\theta_c(r,\phi)} \sin\theta \cos\theta \, d\theta}{\int_0^{\pi/2} d\phi \int_0^{\theta_c(0,\pi/2)} \sin\theta \cos\theta \, d\theta} \tag{2-22b}$$

where in the numerator,

$$\sin^2\theta_c(r,\phi) = \frac{n^2(r) - n^2(a)}{1 - (r/a)^2 \cos^2 \phi}, \tag{2-22c}$$

and in the denominator,

$$\sin^2 \theta_c(0,\pi/2) = n^2(0) - n^2(a) = n_1^2 - n_2^2. \tag{2-22d}$$

Telecommunication-grade multimode fibers have parabolic (or nearly parabolic) profiles, so $g \cong 2$. In that case, the near field becomes

$$\frac{P(r)}{P(0)} = \sqrt{1 - (r/a)^2}. \tag{2-23a}$$

If leaky rays are excluded,

$$\frac{P(r)}{P(0)} = 1 - (r/a)^2. \tag{2-23b}$$

The far field of the fiber can be obtained similarly from eq (2-22b) by again assuming all modes are equally excited and $g = 2$:

$$\frac{P(\theta)}{P(0)} = \int_0^{R(\theta,\phi)} \int_0^{\pi/2} R\,dR\,d\phi,$$

where $R = r/a$ and, for leaky and guided rays,

$$R^2(\theta,\phi) = \frac{1 - [\sin\theta/(NA)_o]^2}{1 - [\sin\theta/(NA)_o]^2 \cos^2\phi}. \tag{2-24a}$$

When leaky rays are excluded,

$$R^2(\theta,\phi) = 1 - [\sin\theta/(NA)_o]^2. \tag{2-24b}$$

For $g = 2$, the fiber far field is

$$\frac{P(\theta)}{P(0)} = 1 - \left(\frac{\sin\theta}{(NA)_o}\right)^2 \tag{2-25a}$$

for bound modes only and

$$\frac{P(\theta)}{P(0)} = \left[1 - \left(\frac{\sin\theta}{(NA)_o}\right)^2\right]^{1/2} \tag{2-25b}$$

when leaky rays are included.

The LPS launch calls for a uniform launch spot of specified size and specified launch angle. These conditions can be put into perspective by using the concepts discussed here. Consider a uniform spot of diameter r_o focused onto the end of a fiber core having diameter a. The launch angle with

respect to the fiber axis is θ_o. The power that the spot launches into the fiber can be found using eqs (2-4), (2-9), and (2-10). The radial and azimuthal coordinate variables in the plane of the fiber end face (or spot) are taken to be r, ξ. Incremental area da is therefore r dr dξ. The total power coupled from the spot to the fiber is

$$P(r_o,\theta_o) = \int_0^{r_o} \int_0^{\theta_o} \int_0^{2\pi} \int_0^{2\pi} L \, r dr d\xi \sin\theta \cos\theta \, d\theta d\phi \qquad (2\text{-}26a)$$

where L is the (uniform) radiance of the launch spot and $\sin\theta \, d\theta d\phi$ is the solid angle into which da launches power (cf. fig. 2-5, but r and ξ are not shown in that figure). da $\cos\theta$ is the component of da that is normal to the ray direction. We suppose that the launch spot radiance is independent of ξ, yielding

$$P(r_o,\theta_o) = L_o(\pi r_o)^2 \sin^2\theta_o. \qquad (2\text{-}26b)$$

In deriving this equation, we have assumed that the fiber accepts all rays incident from the launch spot. The validity of this assumption depends on the refractive index profile of the fiber. If the fiber has a parabolic profile, the assumption will hold if r_o and θ_o are related thus:

$$(r_o/a)^2 + [\sin\theta_o/(NA)_o]^2 \leq 1, \qquad (2\text{-}26c)$$

with $(NA)_o$ defined in eq (2-15).

Additional insight is had by normalizing eq (2-26b), using $R_o = r_o/a$:

$$P(R_o,\theta_o) = KR_o^2\left[\frac{\sin\theta_o}{(NA)_o}\right]^2, \qquad (2\text{-}26d)$$

where K is a constant that depends on the strength of source. The LPS launch is based on a meaningful choice of R_o and θ_o. This is discussed further below.

Equation (2-26d) is a measure of how well the phase space of the spot matches that of the fiber. In this sense, it gives the expected coupling efficiency between the two but without including reflection loss. This will be seen in discussing figure 2-6c, which is a plot of eq (2-26d). Equation (2-26d) is fundamental to the LPS launch, since it contains only the launch spot parameters and the fiber parameters.

Figures 2-6a, b, c, and d are plots of eqs (2-13), (2-23), (2-25), and 2-26d) subject to eq (2-26c) for g = 2. They are included to help explain the LPS launch. Note first that the straight diagonal line between (0,1) and (1,0) in the figures is the line $y^2 = 1 - x^2$, where y^2 is the ordinate and x^2 is the abscissa. The region below that line represents the region of bound modes. Figure 2-6a shows that if the launch spot size is 70 percent of the fiber core size and the launch numerical aperture is 70 percent of the fiber numerical aperture, the phase space excited in the fiber is shown by the square in the lower left corner of the figure. The power launched is given by eq (2-26d) with $R_o^2 = 0.5$ and $[\sin\theta_o/(NA)_o]^2 = 0.5$. No leaky modes are excited.

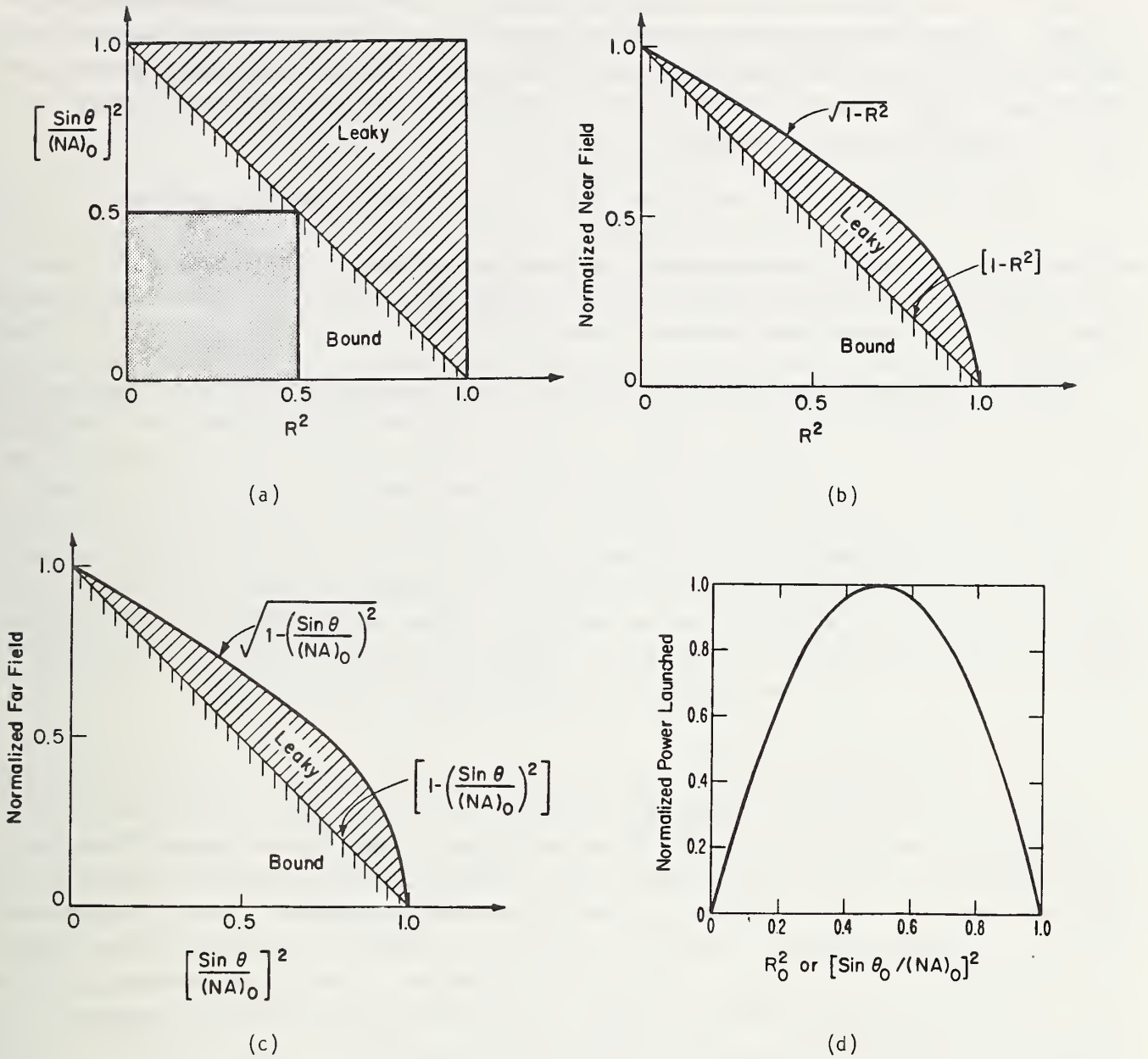

Figure 2-6. (a) The phase space of a graded-index fiber. Darkened area shows the phase space excited by the LPS launch.
(b) The normalized near field of a parabolic profile fiber (g = 2).
(c) The normalized far field of a parabolic profile fiber (g = 2).
(d) Normalized power launched into a parabolic profile fiber (g = 2) under the condition that R_0 and $\sin\theta_0$ are chosen so no leaky modes are excited but that maximum power is coupled into the fiber. Uniform launch condition.

Holmes [9] has discussed the launch condition described here. He defined the EMV (effective mode volume) of a fiber in terms of the far-field and the near-field intensity distributions of the fiber. EMV is the square of the product of the normalized full width at half maximum (FWHM) of the near-field distribution and the normalized sine of the half width at half maximum (HWHM) of the far-field radiation pattern. Figures 2-6b and 2-6c relate this definition of EMV to the LPS launch condition illustrated in figure 2-6a. If leaky rays are excited, the near field and the far field will reveal this. Defining EMV in terms of the far field and the near field is thus obviously related to the modal power distribution, as seen from the figures.

EMV is a convenient device and has proved to be useful in predicting steady-state conditions of the fiber. Once the modal power distribution of a fiber is in equilibrium, the EMV as measured at the fiber output is independent of fiber length; this is the condition sought when predicting attenuation of concatenated links. The EMV at the input of a fiber depends on launch spot size and launch numerical aperture as shown in the figures.

The concept of EMV is helpful and its use led to a useful launch condition. Recent work demonstrates the complexity of the problem, however, and EMV clearly is not sufficient to circumscribe the variabilities in attenuation measurements. A comparison of several filters and/or mode mixers shows that each has its limitation but fortunately the fiber attenuation is relatively insensitive to the fine details of launched modal power distribution [12,13].

Figure 2-6d relates the 70-70 launch condition to power launched under the restriction that spot size and launch numerical aperture are chosen so no leaky modes are excited but that power coupled into the fiber is maximum. This maximum power condition is not the primary reason for selecting the 70-70 launch condition. It does represent a happy coincidence, however.

Figure 2-7 [14] further illustrates the reason for the limited launch. The figure gives attenuation along the vertical axis with launch variables in the horizontal plane. The measured attenuation depends on how effectively various modes are excited. If the fiber core and numerical aperture are fully filled at launch, attenuation is skewed by the high-loss modes, giving results that would not be useful in predicting the loss in a system of several kilometers length.

2.1.1 A Summary of Phase Space Concepts

The definitions and connecting relationships given above form the basis of fundamental and important concepts in optical coupling, including the coupling of light energy between a source and a fiber. Phase space is a four-dimensional space that is defined in terms of geometrical optics and light rays. Two of the four dimensions are associated with the momentum of a ray [eq (2-1)] and the other two are associated with the ray's spatial position. Each point in the four-dimensional space has a one-to-one relationship to the ray's position in space and its direction (or momentum). This is important because a ray enters a fiber at a point in space (on the fiber core) with a momentum determined by its angle with respect to the fiber axis [cf. eq (2-2)].

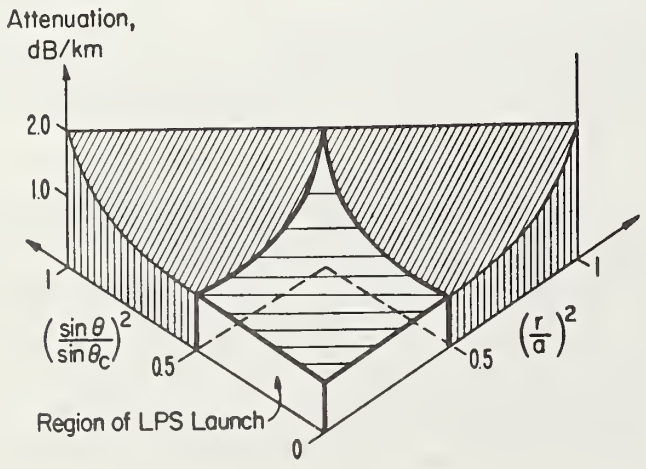

Figure 2-7. Attenuation as a function of ray parameters (after ref. 14).

The ray is bent as it passes from air into the fiber core according to Snell's law. The bending can be described in terms of phase space by invoking the concept of the density of points in phase space, denoted above by ρ. Neither the density of points nor the volume enclosing a fixed number of points in phase space can change with z, the axial coordinate. Snell's law is a direct result of this conservation principle. The conservation of density (ρ) and of volume (ψ) is a manifestation of Liouville's theorem in statistical mechanics. The conservation of radiance is a consequence of these conservation principles [see eq (2-12)].

Equation (2-9) shows that incremental volume in phase space is the product of area, solid angle, and the square of refractive index. [The refractive index is squared because the angle is two dimensional (solid).] It is precisely this product that is controlled in the LPS launch. The product is conserved in going from air to fiber core. The product is also the determinant of power launched into the fiber. That is the thrust of eqs (2-13) to (2-26), as illustrated in figures 2-6(a) to 2-6(d).

Equation (2-26a), when used in conjunction with figure 2-6(a), can be used to deduce power coupled into a fiber under several conditions. When a uniform source is assumed, the calculation can be done easily in closed form. The figure helps in defining limits of integration. In particular, if a spatially uniform light spot of radius r_o is focused onto the end of the fiber, the total power coupled into the fiber (neglecting reflection losses) is

$$P = 2\pi \int_0^{r_o} r\,dr \int_0^{\theta_o} \int_0^{2\pi} \sin\theta \cos\theta \, d\theta \, d\phi,$$

where θ_o is the limiting value of θ; several values of θ_o and r_o will now be considered.

If the fiber is filled, $r_o = a$, $\theta_o = \theta_c$ as given in eq (2-22c). The corresponding value of P will be referred to as P_{TOT}. For the LPS launch, $\sin^2\theta_o = (NA)_o^2/2$ and $r_o = a/\sqrt{2}$ (cf. fig. (2-6a)). The corresponding power launched will be referred to as P_{LPS}. The power coupled into guided modes, to the exclusion of leaky modes (referred to below as P_g), is found by taking $\sin^2\theta_o = (NA)_o^2[1 - (r/a)^2]$ and $r_o = a$. To complete the picture, we will refer to $P_g - P_{LPS}$ as $2P_d$. The region outside the shaded square but below the straight diagonal line in figure 2-6(a) represents the power $2P_d$. Finally, the amount of power in the leaky modes (P_ℓ) is $P_\ell = P_{TOT} - P_g$. The following relationships are obtained from the integration, assuming a parabolic fiber with uniform mode excitation.

$$P_g/P_\ell = 3, \tag{2-27a}$$

$$P_g/P_{TOT} = 3/4, \tag{2-27b}$$

$$P_\ell/P_{TOT} = 1/4, \tag{2-27c}$$

$$P_{LPS}/P_{TOT} = 3/8, \tag{2-27d}$$

$$P_d/P_{LPS} = 1/2. \tag{2-27e}$$

These ratios will be used later.

Equation (2-26d) gives the power coupled into a parabolic profile fiber as a function of launch spot size and launch angle. It is again the product of area and solid angle that is the determinant of power launched. The equation shows that launching power is a matter of matching the phase space of the source to the phase space of the fiber. Only the phase space of each (aside from a multiplying constant) appears in the equation. The maximum value of the right hand side is K and that obtains when the phase space of the source equals that of the fiber; i.e., the fiber is filled and all bound modes are excited. In that case, $R_0 = 1$ and $\sin\theta_0 = (NA)_0$.

The equations reveal an interesting picture of power coupled into the bound modes of a parabolic fiber. If launch angle and launch spot size are independently adjusted so only bound modes are excited, then maximum power is coupled into the fiber when launch spot diameter is 70 percent of core diameter and launch numerical aperture is 70 percent of fiber numerical aperture, provided the launch spot is in focus and exactly centered on the fiber core.

Finally, the connecting relationships and figure 2-6 lead to what has been called the EVM (effective mode volume) of a fiber [9]. EMV is defined as the square of the product of the full width at half maximum of the near-field pattern and the half width at half maximum of the far-field pattern. That this is so is discussed above. Thus, the 70/70 launch condition is based on both the near field and the far field of the fiber. The mode filter launch, described later, is based only on the far-field pattern of the fiber. The question of equivalence of the methods arises naturally, then. The question cannot be answered definitely but some intuitive arguments in this regard are given later.

2.2 LPS Launch

Figure 2-8 is a block diagram of the system used to control launch spot size and launch numerical aperture independently, in accordance with the requirements of the LPS technique. The method is sometimes referred to as the beam optics method of launch.

The light source is a tungsten strip lamp powered by a regulated power supply to maintain stability during the measurement. The strip lamp is preferable to coiled filament lamps because it produces a spatially uniform spot. The lens L_1 converts the diverging beam to a beam of parallel rays that pass through the interference filter for wavelength selection. The filters have a 10 nm spectral width. The wheel that houses the several filters allows white light as one option; this option can be used for alignment, as occasionally required. Lens L_2 focuses the beam onto the aperture A_1, called the source aperture, which is imaged onto the specimen. The size of A_1 can be changed to adjust the launch spot size.

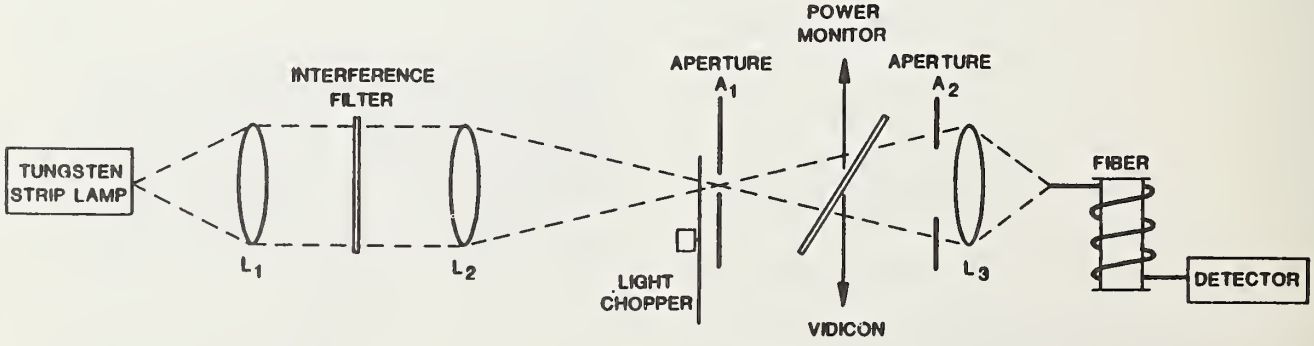

Figure 2-8. Block diagram of attenuation measurement system. The system allows launch spot size and launch numerical aperture to be controlled independently.

The beamsplitter shown in the figure serves a dual purpose. First, the arm marked power monitor goes to a reference detector which monitors the stability of the light source. Correction can be made in the final results if the output light power drifts during measurement. Experience has shown that with a stabilized power source for the lamp, correction is almost never required and measurements are often made without the monitor arm activated. The computer program that controls data acquisition allows the operator to monitor the source or not, as he sees fit. The beamsplitter also allows viewing the fiber end with the vidicon.

Aperture A_2 controls the launch numerical aperture by restricting the beam angle. Thus, A_1 and A_2 must both be adjustable, in accordance with the needs of the LPS launch.

The magnification ($m < 1$) introduced by the optics between A_1 and the fiber end must be known. The spot size on the fiber end is determined from m and the size of A_1. The launch spot size (A_L) is:

$$A_L = A_1 (\ell_3/\ell) = mA_1,$$

where ℓ_3 is the distance from L_3 to the image plane and ℓ is the distance from A_1 to L_3. Dimensions are not accurately known so m is determined by measurement. A pinhole detector (small compared to expected spot size) scans the image plane of L_3 to measure launch spot size for a known size of aperture A_1. Magnification is then calculated. In a similar manner, the launch NA effected by aperture A_2 is determined by measuring the far-field beamwidth as a function of aperture size. A catalog is thus easily established, allowing for selection of A_1 and A_2 to meet the needs of the LPS launch method. Commonly accepted tolerances on A_L and launch NA are as follows:

$$A_L/d = 0.707 \pm 0.05 \tag{2-28}$$

$$\frac{\text{launch NA}}{\text{fiber NA}} = 0.707 \pm 0.05 \tag{2-29}$$

where d is nominal fiber core diameter.

The launch NA called for in eq (2-29) is measured at distances considerably greater than $10\ d^2/\lambda$, which is the usual definition of far field. The launch angle is obtained from geometry, knowing the distance from the focal plane of L_3 to the measurement plane and having obtained the measured beamwidth at that plane. The distance from the focal plane of L_3 to the measurement plane is accurately known because the detector is mounted on a micropositioner stage.

The standard cut-back technique is used to calculate fiber attenuation from the measured values of power; see eq (1-3). An alternative technique, also based on the cut-back technique, can be used if the fiber ends are prepared with suitable care and input alignment is carefully controlled. In this case, a short piece of the fiber under test is prepared in advance, as is the test fiber. A two-fiber bed on a translation stage allows the input to be focused alternately on the short fiber and the test fiber. The two fibers are likewise coupled to the detector so one can measure the power transmitted through the short piece or the test fiber, alternately and conveniently. The ratio of the two readings gives attenuation, but the technique depends on good agreement in the input coupling for the two fibers. Such agreement is especially important in low-loss fibers, for which a true cut-back technique is preferred. In this one-fiber technique, the input end (which is the more critical end) is unchanged in the course of the measurement. Thus, the modal power distribution established at

launch is the same for both measurements. The two-fiber method allows input coupling errors on two counts. First, the preparation of the two fiber ends may differ, even though slightly, allowing for differences in input coupling loss. Second, the alignment may differ, leading to a difference, however slight, of the launched modal power distribution. These two effects may be cumulative, leading to inconsistent power readings and unreliable loss values. With the true cut-back technique, using only a single fiber, the input coupling efficiency and modal power distribution are the same for both test and reference fiber power measurements.

2.3 Mode Filter Launch

The purpose of defining a standard launch condition is to simulate a fiber having an equilibrium modal power distribution. The measured attenuation will then allow prediction of the attenuation expected in field installations, where long fibers are encountered and an accurate prediction of system loss is essential. Linear addition of attenuation is crucial and will be possible only if the measured attenuation for a test fiber is based on steady-state or equilibrium conditions.

Both the LPS launch and the mode filter launch yield results that scale linearly with distance [10]. Both launch conditions were used for attenuation measurements reported in this document.

A mode filter is a device used to select, reject, or attenuate a certain mode or modes [11]. A mode scrambler is a device for inducing mode coupling in an optical fiber [11]. Our purpose is to establish the equilibrium modal power distribution; i.e., the power distribution that prevails at the end of the long test fiber. Whether the modes are filtered or scrambled is thus an academic question. In fact, workers do not agree on just how the equilibrium state is established [2,12,13] or how best to accomplish the desired end. Reference 13 indicates that modal power distribution is affected in different ways by different filters and scramblers on different fibers.

The method of the mode filter launch is based on the assumption that the relative modal power distribution at the end of a long fiber without the mode filter is the same as it is at the end of a short reference fiber with the mode filter in place. Furthermore, the method assumes that the far-field radiation pattern is a suitable indicator of whether or not the modal power distributions are, in fact, the same. If those patterns are the same, or nearly so, the mode filter has served its purpose, having eliminated certain modes and induced an equilibrium modal power distribution which is equivalent to that at the end of a long fiber.

The mode filter probably does more than just eliminate certain high-order modes. It may induce mode coupling as well, to establish a balance between intermodal power transfer and modal attenuation. The primary function of the filter, however, is to eliminate the high-order modes.

The power distribution in the far field of a fiber depends on modal power distribution. If all modes carry the same power, then each incremental area of the core cross section at the fiber end will uniformly illuminate its cone of acceptance. Therefore, all areas on the fiber core that have a local numerical aperture greater than $\sin\theta$ will contribute equally to the far-field power at angle θ, where θ is the angle between the fiber optical axis and the reference point in the far field. The far-field pattern is therefore a function of fiber numerical aperture. In practice, mode coupling and mode-dependent loss lead to unequal power distribution among the modes at the output end of the fiber. In that case, not all modes contribute equally to the power at angle θ. Nevertheless, the far-field

pattern width is still a measure of fiber numerical aperture, although the specification of how pattern width is defined now becomes a consideration.

In the mode filter method, the adequacy of the mode filter is based on a comparison of the far-field patterns of two fibers (the test fiber without a filter and the reference fiber with the filter). If the angles agree at the 5 percent intensity points, modal power distribution is assumed to be approximately the same.

The mode filter is qualified as follows. Power is launched into the long test fiber with a spot size greater than the fiber core size and with launch numerical aperture greater than the fiber numerical aperture. This will be refered to as overfilling the fiber. The far-field radiation pattern is then measured, where far field means distances greater than 10 d^2/λ from the fiber end, and where d is fiber core diameter. A short reference fiber is then prepared for the purpose of "qualifying" the mode filter. The reference fiber is overfilled and then subjected to the mode filter. The far-field radiation pattern of this reference fiber is measured and the mode filter is adjusted to produce a far-field pattern which is equivalent (within tolerance) to the pattern of the long fiber without the filter. The filter is deemed acceptable if the pattern widths are the same at the 5 percent intensity points. The tolerance is given below [eq (2-30)].

The procedure uses the arrangement shown in figure 2-9 [15]. A filter is normally qualified for only one fiber. Changing the test fiber usually calls for a change (even though slight, in some cases) in the filter. Once the filter has been qualified, attenuation is measured using simple launch optics. The fiber is overfilled and the filter is in place for power measurements on both the long test fiber and the short reference fiber, to insure that the insertion loss of the filter is accounted for.

Workers have used several forms of mode filter, including dummy fibers, macroscopic-bend mandrel wraps and serpentine bends [16]. The measurements reported in this document were taken with a serpentine bend filter, which is shown schematically in figure 2-10. This design is similar to that used by other workers [17]. The filter consists of 7 nylon posts, each of 1 cm diameter. The posts are on 1.3 cm centers. Three of the posts are on a translation stage, allowing for movement of those posts to adjust the strength of the filtering.

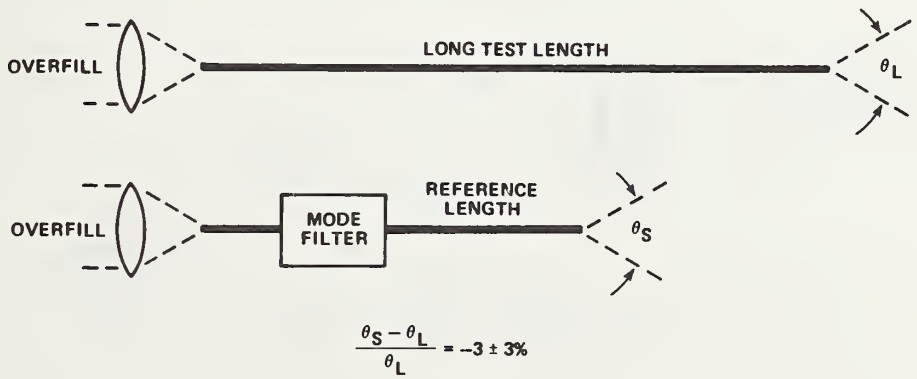

Figure 2-9. Arrangement for qualifying a mode filter.

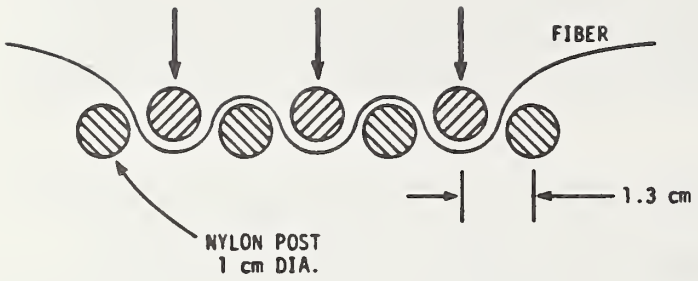

Figure 2-10. Mode filter used for measurements reported herein.

The mode filter technique requires knowledge of θ_L (see fig. 2-9); θ_S is then measured using a short length of reference fiber taken from the spool of test fiber. Moving the posts of the filter (fig. 2-10) changes the angle θ_S. The requirement is [18]

$$\Delta\theta = \frac{\theta_S - \theta_L}{\theta_L} = -0.03 \pm 0.03. \qquad (2\text{-}30)$$

The equation is defined so $\Delta\theta$ is not positive. A negative value for $\Delta\theta$ results from excessive filtering. In that case, the mode filter causes θ_S to be slightly smaller than (or, at most, equal to) θ_L. Equation (2-30) discourages the acceptance of high-order modes that are known to lead to inaccurate loss measurements. A positive value of $\Delta\theta$ implies inadequate mode filtering.

The experimental arrangement for the mode filter launch is simpler than that for the LPS launch because careful control of the spot size and launch numerical aperture are not required. The fiber must be overfilled and this is easily accomplished without much fuss. A typical experimental arrangement is shown in figure 2-11, where the mode filter is shown as a mandrel wrap [10]. The attenuation measurement technique is as follows (cf. fig. 2-11): After the filter is qualified, it is used in the long test fiber and detector power is measured. The fiber is then cut as shown in the figure and power is measured out of the cut length under the same launch conditions. The ratio of the two powers provides the loss using the cut-back formulas.

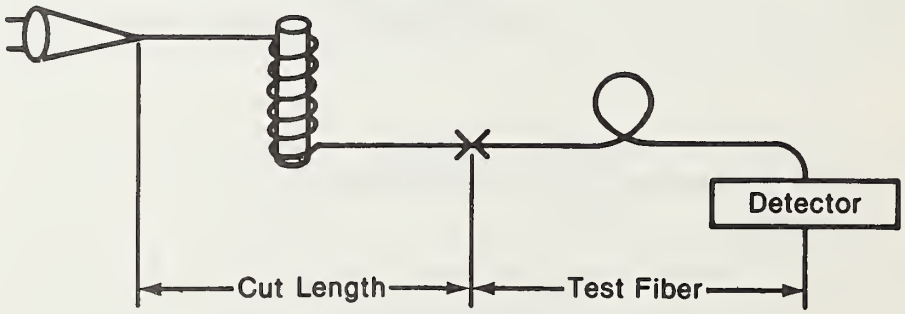

Figure 2-11. Experiment arrangement for attenuation measurement using a mandrel wrap mode filter [12].

That the mode filter launch and the LPS launch should yield comparable loss measurements is not obvious. It seems intuitive that different amounts of power are coupled into the test fiber under the two launch conditions. Furthermore, the LPS launch is based on both near field (launch spot size) and far field (launch numerical aperture) information. The mode filter launch is based entirely on the far field. A question naturally arises then as to whether one can expect the two methods to establish equivalent modal power distributions in the fiber. Most important in this regard is the attenuation or elimination of high order and leaky modes. Either method is effective in this regard. Beyond that, however, we are forced to conjecture on the similarities of the two methods. Figure 2-6a is useful in visualizing concepts. The darkened area is proportional to power launched under the LPS method. That area represents the product of physical area and angle, as already discussed. According to eq (2-27d), the ratio of power carried by a fully filled fiber (including leaky modes) to that carried by a fiber filled at the 70/70 level (P_{TOT}/P_{LPS}) is 2.67 or 4.26 dB. If a mode filter eliminates the leaky modes from the filled fiber, the ratio reduces to 3 dB $[(P_{LPS} + 2P_d)/P_{LPS}]$. Thus, the ratio of power launched into an overfilled test fiber with a mode filter to that launched using the LPS method is 3 dB or possibly less. If the mode filter introduces additional loss (which is assuredly the case), the figure will be less than 3 dB.

The mode filter almost certainly does more than just eliminate the leaky rays. It probably attenuates the high-order modes and encourages modal power coupling as well. This seems obvious from the fact that the filter must restrict the far-field pattern of the fiber in order to be acceptable. It seems reasonable, then, to suppose that the mode filter eliminates power associated with the following regions of figure 2-6a:

$$0.5 < \left(\frac{\sin\theta}{\sin\theta_c}\right)^2 < 1 - (r/a)^2 \tag{2-31}$$

and

$$1 - (r/a)^2 < \left(\frac{\sin\theta}{\sin\theta_c}\right)^2 < 1. \tag{2-32}$$

If so, the ratio of power launched with a mode filter to that launched using LPS is $(P_{LPS} + P_d)/P_{LPS}$ or 1.76 dB (see eq (2-27e)). This assumes that the filter does not attenuate low-angle rays. It further assumes that the rays specified by eqs (2-31) and (2-32) are completely eliminated. A laboratory measurement of power launched into a fiber using the mode filter and the LPS launch yielded a ratio of 1.64 dB.

If what we suggest here is true, then the two launch conditions will yield comparable loss measurements even in fibers having differential mode attenuation. If a fiber has very little differential mode attenuation, the two methods will yield comparable results even if what we suggest is not true.

Appendix A relates these concepts to the fiber mode volume. The latter term is a popular one that is easy to understand since it identifies the number of modes that a fiber can support. Appendix A shows that the ratio of the total number of guided modes supported by a parabolic fiber to the number supported between $r = 0$ and $r = a/\sqrt{2}$, is 1.25 dB. Thus, the preceding discussion suggests that the mode filter may eliminate all of the leaky modes but couples some of the energy into low-order guided modes.

3. Component and System Variabilities

The measurement system shown in figure 2-8 will yield meaningful results only if the conditions of the restricted launch (either LPS or mode filter) are met. That they are met is confirmed through measurement. The variabilities encountered in measuring the pertinent parameters are discussed in this section. In addition, linearity and noise are discussed for the dynamic range and wavelength range of interest in the current telecommunications-grade fiber market.

The measurement of magnification (denoted m and discussed in the following section) allows a prediction of launch spot size for a known aperture size A_1. The measurement of m and of launch numerical aperture require the measurement of beam widths. Unfortunately, there are fundamental limits to the accuracy with which one can measure those widths. The limits are imposed by virtue of diffraction and the finite size of the detector aperture.

A similar limit is imposed in qualifying the mode filter. The patterns being measured invariably have sloping skirts which make it difficult to clearly define the 5 percent points of the pattern.

This section also addresses the question of component and system linearity and system noise. For fibers of interest today, the required dynamic range is only a few decibels so acceptable linearity is easily attained. System noise is well below the level of tolerance.

3.1 Spot Size and Launch Numerical Aperture

Independent adjustment of launch spot size and launch numerical aperture is accomplished using apertures A_1 and A_2 of figure 2-8. The diameter of the spot focused onto the end of the fiber is the magnified diameter of A_1, where the magnification m is approximately

$$m = f_3/\ell \tag{3-1}$$

where ℓ is the distance from A_1 to L_3 and f_3 is the focal length of L_3. Although m is defined here in terms of distances, in practice it is experimentally determined since ℓ is not known accurately. m is found by measuring the launch spot size (mA_1) using a large aperture. The variation of m with wavelength is shown later. The diameter of A_1 is determined by visual examination using a microscope with a two-dimensional vernier stage to identify edge location.

Measurement of m is accomplished by placing a small aperture in front of a detector and in the image plane of L_3. The combination is scanned across a diameter in that plane to determine spot size. Knowing the size of A_1 then allows the calculation of m.

If the focused image of the aperture had spot has perfectly sharp edges, sweeping the detector aperture through that spot could be described by the convolution of two cylinder functions $CYL(r/d_s) * CYL(r/d_a)$, as shown in figure 3-1, where

$$CYL(r/d) = \begin{cases} 1 & , 0 \leq r < d/2 \\ 1/2, & r = d/2 \\ 0 & , r > d/2 \end{cases} \tag{3-2}$$

where d_s and d_a are the diameter of the spot and the aperture and * denotes convolution.

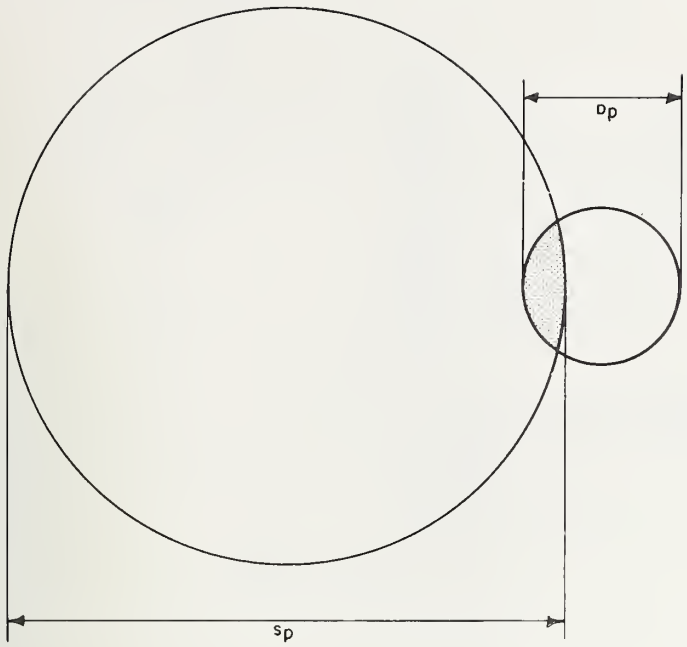

Figure 3-1. Two cylinder functions, representing an aperture and a spot being measured.

The cylinder function is an accurate description of the transmittance of the circular aperture over the detector but the focused spot invariably has skirts, owing to diffraction. Nevertheless, it is instructive to consider the case of perfectly sharp functions to describe both the spot intensity (in the focal plane of L_3) and the aperture. To estimate potential errors encountered in the system, and to define the "small aperture" alluded to earlier, we consider a one-dimensional problem, the convolution of two rectangular functions, one of width w_s and one of width w_a, where the subscripts refers to spot and aperture; we take $w_s > w_a$. The functions and their convolution are shown in figure 3-2. This figure shows that the accurate measurement of w_s is difficult. The measured form (fig. 3-2c) differs from the actual spot (fig. 3-2a) by an amount that depends on w_a. The FWHM of figure 3-2c differs from that of figure 3-2a by w_a.

Clearly, we require $w_a \ll w_s$. If w_a is a delta function, the spot is reproduced exactly in the measurement. However, as w_a is decreased to improve the measurement precision, the signal-to-noise ratio is decreased. Obviously, the measurement of launch spot size calls for a compromise in the name of accuracy. w_a should be as small as possible, commensurate with the need for acceptable signal-to-noise ratio.

Since total measured width is proportional to $w_a + w_s$, the allowed value of w_a is proportional to allowed error on measured w_s. For 1 percent error, w_a must be not more than 1 percent of w_s. If the spot size is defined at the 10 percent intensity points, w_a can be slightly larger: $w_a < 0.0125\ w_s$. The convolution suggested by figure 3-1 does not differ substantially from that shown in figure 3-2, if $d_a \ll d_s$.

This simple approach, based on rectangular functions in one spatial dimension, is useful because it is intuitive. In practice, the measured spot is the convolution of a cylinder function and a two-dimensional function which accounts for diffraction.

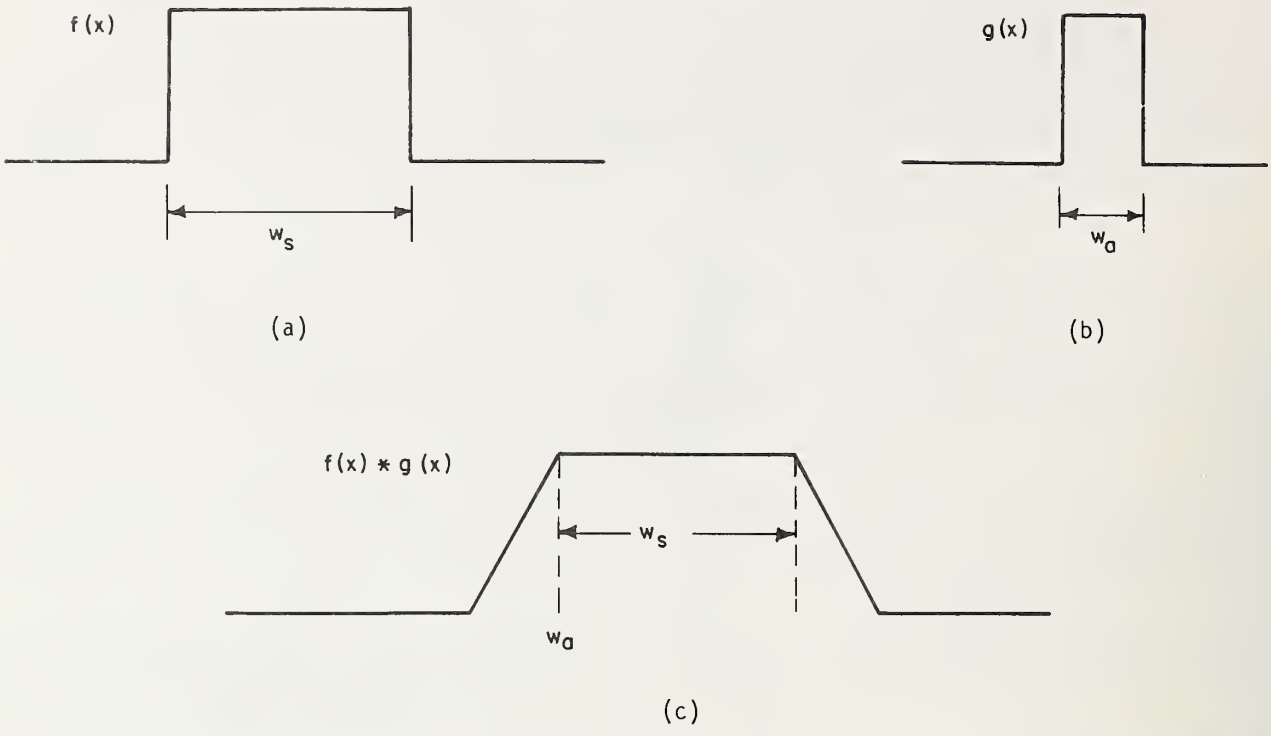

Figure 3-2. The convolution of two rectangulr functions, illustrating the error introduced when measuring f(x) (a) using an aperture g(x) (b) resulting in f(x) * g(x) as shown in (c).

Figure 3-3 shows the measured spot in the focal plane of L_3 with A_1 = 3012 μm at 850 nm, with a 1 μm aperture over the detector. The width at the 10 percent intensity points is 140 μm, indicating that

$$m = 1/21.6. \tag{3-3}$$

Figure 3-4 shows how magnification changes with operating wavelength. Obviously, the chromatic aberrations of the intervening lenses and the beamsplitter are not excessive. Variation of m over the range measured is ±0.1 or about 0.5 percent. If the fiber core diameter is 50 μm, the launch spot size should be 35 μm. Invoking the ±5 percent allowance on spot size yields

$$702\ \mu m \leq A_1 \leq 810\ \mu m. \tag{3-4}$$

To determine spot size, the vernier of the translation stage that holds the detector is read at the appropriate signal levels.

The magnification is not expected to change with LNA. The accuracy with which one can measure spot size, however, is a function of the size of A_2 (LNA). Figure 3-5 shows measured values of m as a function of the f-number of the lens L_3. This variation is due primarily to loss of resolution.

The method used to determine LNA can be described with the help of figure 3-6. The source image refered to in the figure is the image of aperture A_1. The source image is in the image plane of L_3. A plane at distance ℓ from the source image is in the far field of that image plane.

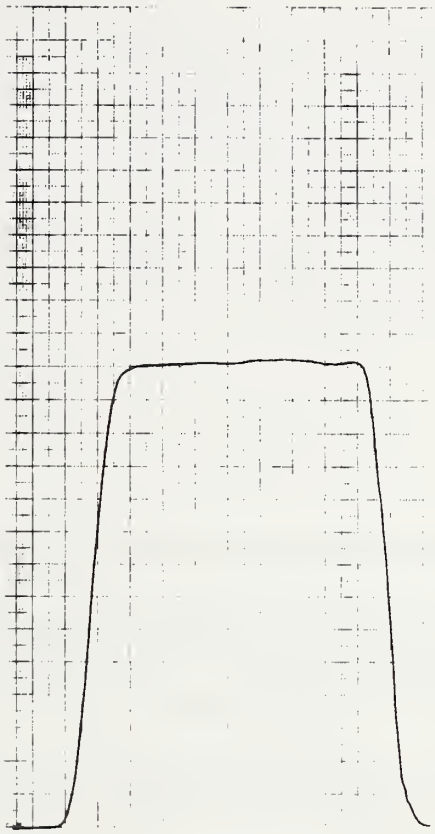

Figure 3-3. Measured spot in the focal plane of L_3.

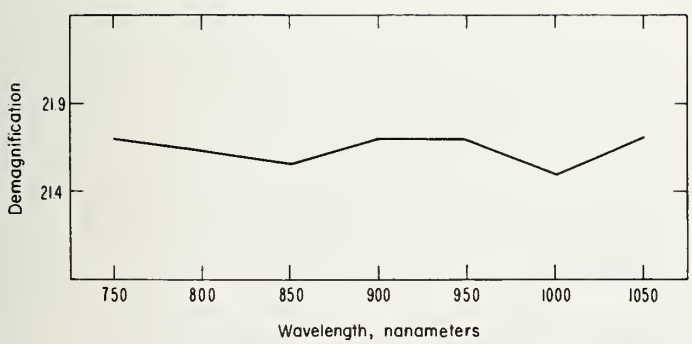

Figure 3-4. Change of demagnification with wavelength.

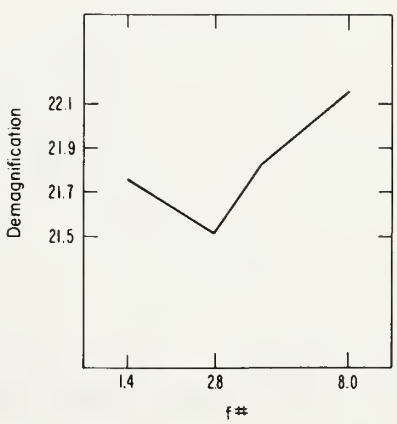

Figure 3-5. Change of demagnification with f# (aperture size).

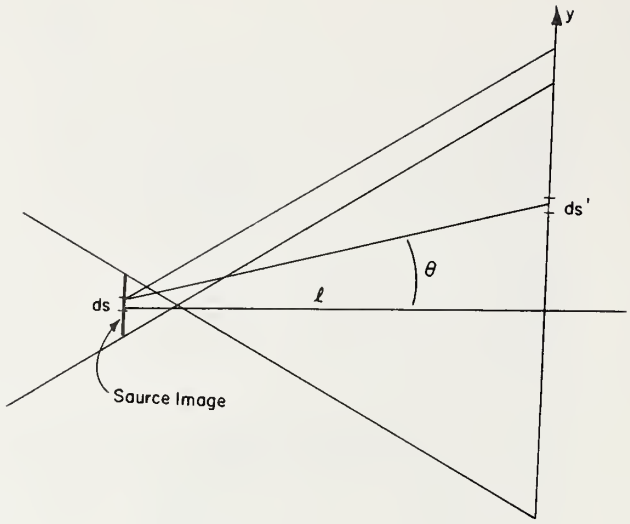

Figure 3-6. Geometry and angles encountered in measuring LNA.

Launch numerical aperture is calculated from the pattern width in the far-field plane and the value of ℓ. The pattern width is measured by placing a small aperture in front of a detector and sweeping the combination in the plane at distance ℓ from the source image.

The pattern measurement is difficult because the edges are not sharp and the corners are rounded. One source of distortion of the pattern is a $(\cos\theta)^4$ variation owing to simple geometry, as follows. Assume that the radiance at the source image is N. The incremental power at ds', in the far field, is

$$dP = N\ ds\ \cos\theta\ d\Omega, \tag{3-5}$$

where

$$d\Omega = \frac{ds'\ \cos\theta}{(\ell/\cos\theta)^2}. \tag{3-6}$$

Taking

$$N = \begin{cases} N_o = \text{constant for } \theta \leq \theta_{LNA} \\ 0 \text{ for } \theta > \theta_{LNA} \end{cases}$$

$$dP = \frac{N_o\ ds\ ds'\ (\cos\theta)^4}{\ell^2}. \tag{3-7}$$

For ℓ large with respect to source image, the power pattern seen by a pinhole detector is then

$$P = P_0(\cos\theta)^4 \tag{3-8}$$

where P_0 is the on-axis value, which depends on N_0, ℓ, and source size. The pattern is invariably rounded at the edges, because of this $(\cos\theta)^4$ function [19]. For small values of LNA, a binomial expansion of $(\cos\theta)^4$ yields an expression for $P(y)/P(0)$, where y is the rectangular coordinate perpendicular to the optical axis in the plane of measurement:

$$\frac{P(y)}{P(0)} = \left[\frac{1}{1 + \left(\frac{y}{\ell}\right)^2}\right]^2. \tag{3-9}$$

The maximum value of y/ℓ of interest is y_0/ℓ

$$\frac{y_0}{\ell} = \tan(\sin^{-1} \text{LNA}). \tag{3-10}$$

For LNA = 0.2, $P(y_0)/P(0)$ is 0.92 at the edge of the pattern, as shown in figure 3-7. The pattern measured is further distorted because of the finite size of s (fig. 3-8), which causes the skirt shown in figure 3-7. The far-field criterion is therefore

$$\ell >> \frac{S}{2(\text{LNA})}. \tag{3-11}$$

For a fiber having a 50 μm core diameter and 0.2 numerical aperture,

$$\ell >> 125 \text{ μm}$$

is required.

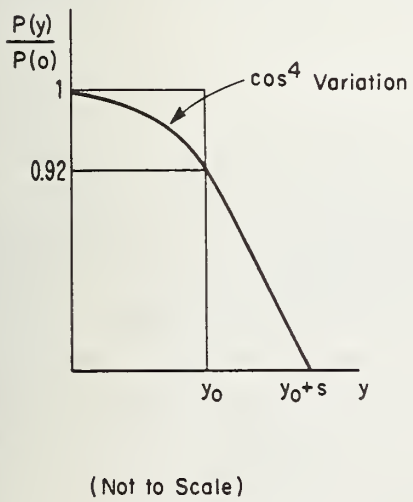

Figure 3-7. Illustrating the distortion of the pattern edge owing to the $(\cos\theta)^4$ variation.

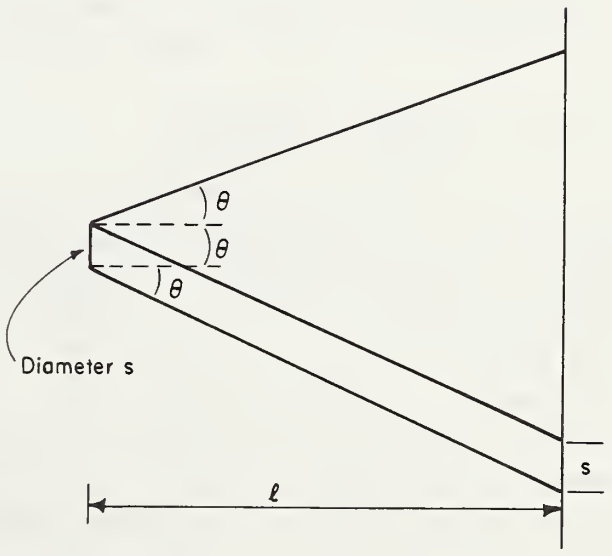

Figure 3-8. Showing the geometry and angles which cause the skirt shown in figure 3-7.

Table 3.1.

f/# or aperture diameter d	Pattern width at 10% points (mm)	LNA
f/# = 1.4	3.72	0.34
f/# = 2.0	2.67	0.25
f/# = 2.8	1.95	0.19
f/# = 4.0	1.41	0.14
d = 3.13 mm	1.42	0.14
d = 6.23 mm	2.89	0.27

Table 3.1 gives the measured values of LNA taken 5 mm from the focal plane. LNA can be changed by changing either the iris diaphragm of the lens L_3 or by placing an aperture in front of L_3 with its diaphragm open. Both techniques were used. The lens diaphragm consists of leaves which mesh together to only approximate a circular aperture. The aperture placed in front of the lens is circular. However, there was no discernable difference in the far-field patterns of the two openings.

The first column of table 3.1 gives the f-number setting of the lens when the lens diaphragm was used to restrict LNA. Lens L_3 has a 12.5 mm focal length. When the f-number setting is 4, then, the diaphragm opening is 3.13 mm. The fourth and fifth rows of the table should be the same. The measured values of LNA do agree to within the measurement precision.

Arbitrary values of LNA can be obtained by adjusting the iris diaphragm on L_3. This was verified by requiring and obtaining LNA = 0.22. The technique is based on the fact that LNA varies linearly with aperture A_2 if the angles are small. In this case, the widths given in table 3.1 were used as the starting points. The aperture was adjusted while observing the intensity on a strip chart recorder. Proportional change of pattern width yielded a proportional change of LNA.

Measurements verify that LNA is independent of spot size. There was no discernable difference in measured LNA for a three-fold change of spot size.

3.2 Mode Filter Qualification

Figures 3-9 and 3-10 show the launch optics and the measurement apparatus used to qualify the mode filter used in the attenuation measurements [20]. A broadband interference filter is used (fig. 3-9) to improve signal-to-noise ratio. The 10 nm filters used in the attenuation measurement do not provide adequate signal level for reliable measurements; the filter used here has an approximately 80 nm spectral linewidth. The measurements are relatively insensitive to wavelength, so the increased linewidth does not affect the interpretation of results. More will be said of this later. Aperture 1 determines launch spot size and aperture 2 controls LNA, as before. The fiber is overfilled for these measurements so the launch conditions are not critical. Alignment is straightforward and based on the criterion of maximum signal. The chopper frequency is set at about 45 Hz. The pattern is measured by using a fixed fiber end and a detector that moves along an arc about the center of the fiber end.

The fiber passes through a cladding mode stripper consisting of two 10-cm long felt pads wetted with index-matching fluid. Any buffer coatings are removed from this part of the fiber. Near-field scans have shown that this type of mode stripper effectively removes light from the cladding.

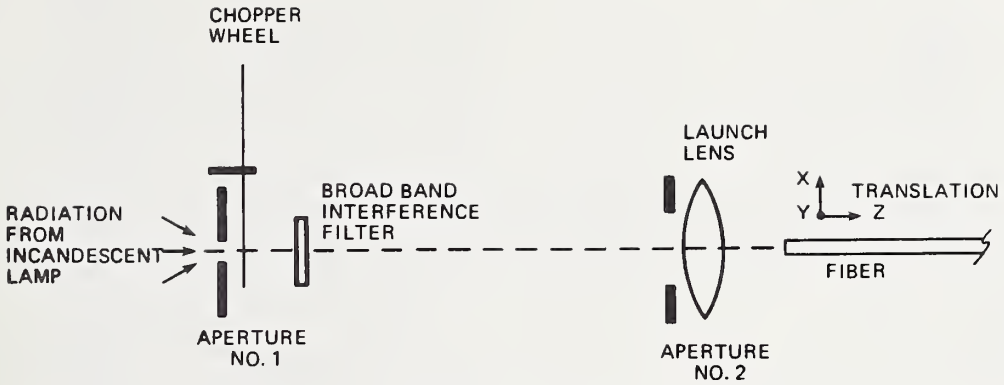

Figure 3-9. Launch apparatus used to measure near field and far field of fiber.

A vee groove positions the fiber to be coincident with the axis of rotation. A small, felt-padded weight holds the fiber in the groove. Before measurement, the fiber end is visually inspected for flatness and perpendicularity. The vee-groove position can be adjusted by a two-dimensional translation stage to assure proper alignment.

Scanning is accomplished with a stepper-motor-controled rotary table, which swings the detector through a 12-cm radius arc. At this distance the far-field criteria is satisfied for core diameters of 100 μm or less. Angular motion (1/2 arc min per step) is fine enough to give smooth far-field curves. Detector aperture size is chosen to give reasonable compromise between resolution and signal-to-noise ratio; the 0.8 mm diameter aperture gives a resolution of 0.38°. A simple one-dimensional model based on a parabolic-shaped far-field pattern with an NA of 0.2 predicts an error of 1.6 percent in radiation angle when the curve is acquired with 0.38° resolution. Measurement precision for determining radiation angle is in the range of 1 to 2 percent when a new output end is prepared and realigned; therefore, a reduction in aperture size would not result in much improvement.

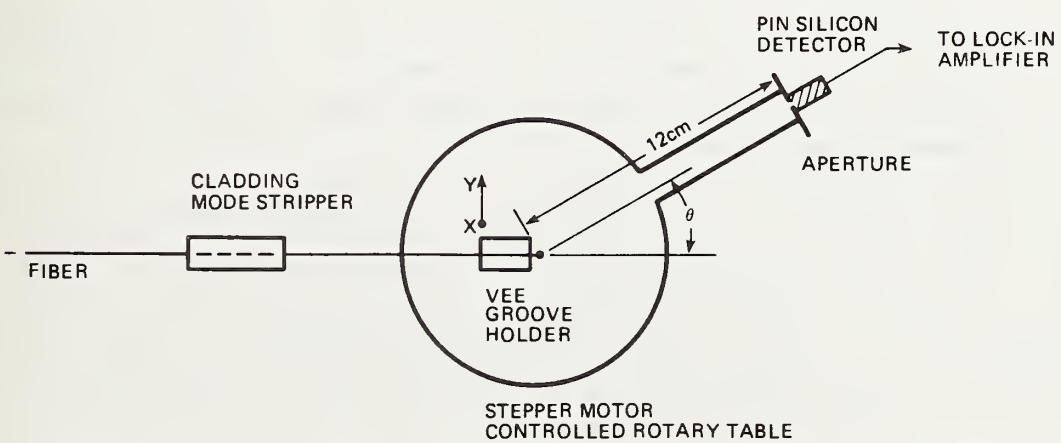

Figure 3-10. Apparatus used to measure fiber far field. The fiber end is fixed and the detector moves along an arc.

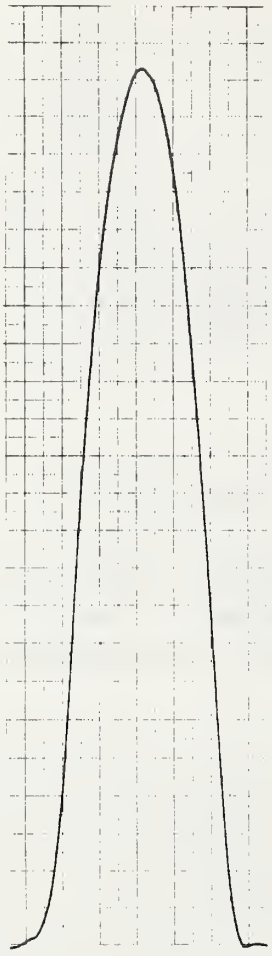

Figure 3-11. Far-field pattern of test fiber 7502 at 850 nm.

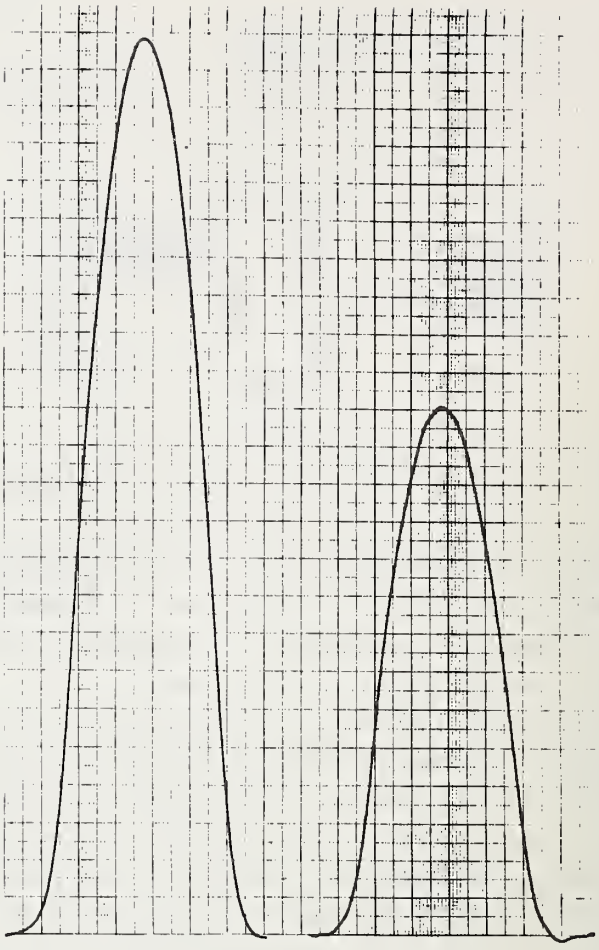

Figure 3-12. Far-field pattern of reference fiber 7502 with mode filter at 850 nm (left) and 1060 (right).

A silicon PIN diode operating in the photovoltaic mode is used as the detector. The detector has an active area of 5.1 mm^2 and a built-in operational amplifier, and is mounted directly behind the aperture. A time constant of 0.4 s is used on the lock-in amplifier. The scanning rate is chosen so one resolution element (0.38°) is scanned in approximately three time constants. At this rate, a far-field pattern is obtained in 3 to 4 min.

The output numerical aperture of a fiber is relatively insensitive to wavelength [21] for the range of interest here. Insofar as this is true, the mode filter need not be requalified for a change of wavelength. To verify this important assumption, a mode filter was qualified at 850 nm and then tested at 1060 nm. The resulting far-field patterns are shown in figures 3-11 and 3-12. There is virtually no difference in the pattern widths. Unfortunately, the signal-to-noise ratio decreases at 1060 nm, making the graph more difficult to read.

If the differential mode attenuation changes with wavelength, the far-field pattern is a function of wavelength. Indeed, any change in the modal power distribution will produce a change in the far-field pattern. If the differential mode attenuation (DMA) is a function of wavelength, a mode filter that is adequate at 850 nm, may not be so at 1300 nm.

Table 3.2.

Indicated full-scale voltage	1000	$1000/\sqrt{10}$	100	$100/\sqrt{10}$	10	$10/\sqrt{10}$	1
Measured full-scale voltage (1000 mV range as reference)	1000	317.2	100.3	31.71	10.03	3.165 ±0.01	0.992 ±0.01
Offset (%)		0.3	0.3	0.3	0.3	0.1	0.8

3.3 Component Linearity

Potential nonlinearities exist at the detector and at the lock-in amplifier/digital voltmeter. Because the reference detector and electronics operate at essentially the same signal levels during measurements on the long and short fibers, nonlinearities in those devices are not likely.

Silicon PIN photodiodes are generally found to be linear at power levels of interest ($\leq$ 10 μW total power). The silicon device used here had previously been calibrated against a calorimetric standard at 1 μW and 1 mW with an apparent difference in responsivity of not more than 0.8 percent.

The linearity of the lock-in amplifier/digital voltmeter combination was determined by comparison with a precision inductive voltage divider. The scale factor for individual scales was constant to 0.1 percent (peak to peak) or better from 3 to 100 percent of full scale for each of the scales most often used, increasing to about 0.9 percent (peak to peak) for the most sensitive scale used and to 3 percent for the most sensitive scale on the instrument. Relative offsets between ranges were also measured and are shown in table 3.2.

This offset error can be avoided by making both measurements on the same scale. A slight adjustment of light power, for example, is often all that is required to insure that a scale change is not required. For our lock-in amplifier, the error encountered in the scale change is about 0.3 percent over most of the range.

3.4 System Linearity

The linearity of the system is most likely to degrade at high intensity points, if at all. System linearity was tested through judicious use of neutral density filters and adjustment of power out of the light source. The test was conducted using narrowband (10 nm) filters to avoid variabilities introduced through the spectrum shift when intensity of the light source was changed. The technique used was as follows: First, a short length of fiber was used to transmit power to the detector. A 2.5 dB filter was then inserted into the launch optics. Attenuation was measured as 2.50 dB. The filter was removed after noting the reading of the DVM (digital voltmeter). The intensity of the light source was then reduced by 2.5 dB so the DVM reading was the same without the filter as it was just before the filter was removed. This represents a new reference reading and the procedure was repeated. The process continues until signal-to-noise ratio is reduced to intolerable limits.

The underlying assumption in this approach is that the attenuation of the filter is independent of power level. Since only relatively low power levels are used, this assumption is reasonable but no

attempt was made to verify it. The measurements were made without changing the scale of the lock-in amplifier. At 850 nm and over a dynamic range of 15 dB, the standard deviation of the filter loss was 0.01 dB or 0.4 percent. The results were confirmed at several wavelengths of interest. The system linearity at 1300 nm was tested over only about 7 dB of dynamic range but the results were the same.

3.5 System Noise

System noise contributes to measurement imprecision, but the level of such noise is usually low. Analysis of the expected noise follows [22]. We adopt the following notation:

A = measured fiber attenuation, dB
V,M = voltage levels at the output of the fiber and the light source monitor, respectively
S(•) = standard deviation
subscript s, ℓ = short and long fibers, respectively.

In terms of V and M, attenuation is

$$A = 10 \log \left[\frac{V_s/M_s}{V_\ell/M_\ell}\right] \tag{3-12}$$

and

$$S(A) = 4.34\left[\left(\frac{S(V_s)}{V_s}\right)^2 + \left(\frac{S(M_s)}{M_s}\right)^2 + \left(\frac{S(V_\ell)}{V_\ell}\right)^2 + \left(\frac{S(M_\ell)}{M_\ell}\right)^2\right]^{1/2}. \tag{3-13}$$

Digitizing noise in the five digit DVM establishes a level of about 10^{-4} for each of the ratios $S(V_s)/V_s$, $S(M_s)/M_s$, $S(V_\ell)/V_\ell$, $S(M_\ell)/M_\ell$. Hence,

$$S(A) \cong 0.001 \text{ dB}. \tag{3-14}$$

For high-loss fibers, $S(V_\ell)/V_\ell$ may limit the dynamic range of the system. Experience has shown, however, that such a limit is not a practical problem since telecommunication-grade fibers of interest seldom have attenuation of more than 3 to 5 dB/km.

Measurement of fibers in the laboratory yielded the following values

$$\frac{S(V)}{V}, \frac{S(M)}{M} \lesssim 5 \times 10^{-3} \text{ at } \lambda = 1300 \text{ nm},$$

$$\frac{S(V)}{V}, \frac{S(M)}{M} \lesssim 5 \times 10^{-4} \text{ at } \lambda = 850 \text{ nm}.$$

The system noise contribution to the standard deviation of the attenuation measurement is therefore about 0.001 dB at 850 nm and 0.01 dB at 1300 nm.

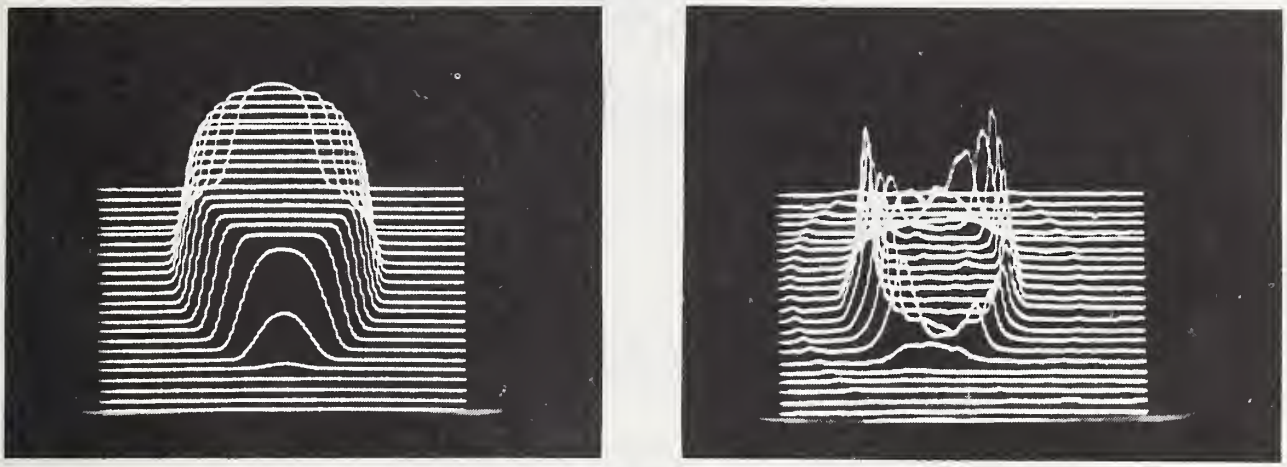

(a) (b)

Figure 3-13. Response of silicon (a) and germanium (b) detectors.

3.6 Detector Uniformity

Figures 3-13(a) and (b) show detector response over the surface of the detector. Figure 3-13(a) is silicon; figure 3-13(b) is germanium. The silicon detector exhibits uniform response, even at its edges. The germanium is uniform over the central region of its surface, but not at the edges. Use of the germanium detector therefore requires more care than does the silicon one. Avoiding the edge is only a minor invonvenience and presents no technical problems. In each case, the detector surface is about 1 cm diameter.

3.7 Measurement Procedure

The cut-back method of measuring attenuation is based on eq (1-3); it calls for the measurement of relative power transmitted through two lengths of the fiber under test. In the notation of eq (1-3), we use L_0 to refer to a short length (the reference length) of the fiber under test; L_1 is the full length of test fiber. The measurement can be performed in either of two ways. To distinguish, we will refer to the first as the two-fiber method; it is suitable for measuring attenuations of more than about 4 to 5 dB. In the two-fiber method, length L_0 is obtained, in advance of any measurements, from the test fiber. Both fibers are prepared and the two input ends are placed on a translatable bed, allowing the light source to be coupled alternatively to length L_0 or L_1, as appropriate. Both output ends are likewise coupled to the detector by placing them side by side on a bed that allows equivalent coupling conditions between the fiber and the detector. In this procedure, care must be taken to ensure that the input ends of the fiber are of similar quality. Input coupling loss can vary, leading to unreliable results if such care is not taken.

In the cut-back method, power transmitted through length L_1 is measured. Without disturbing the launch conditions, the fiber is cut at a point about 2 m from the input, thereby obtaining the reference fiber of length L_0. The cut end is prepared and the power transmitted through L_0 is measured. Equation (3-1) is used in either case to obtain attenuation.

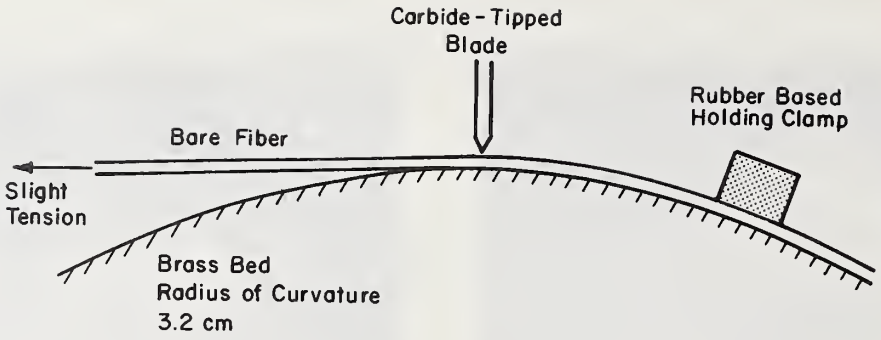

Figure 3-14. Method of cleaving the fiber.

Each of the methods has advantages and disadvantages. The cut-back procedure insures that the long and short lengths are excited with identical launching conditions and also involves the preparation of three rather than four high-quality end surfaces. It therefore is expected to yield better precision, especially with low-loss fibers. The two-fiber procedure, on the other hand, facilitates repeated measurements.

Systematic tests were conducted to determine the sacrifice in precision suffered in using the two-fiber method. The method may introduce as much as 0.1 dB variation in the measured attenuation unless extreme care is taken in preparing the input ends. Only then will input coupling loss be the same for the two fibers. The cut-back method introduces less than 0.03 dB variation in measured attenuation. The output coupling loss is small and is not sensitive to the quality of the cleave, at least if the cleave is reasonably good.

For either measurement method, about 10 cm of bare fiber is required on both ends to accommodate mode strippers. Fiber ends are prepared by scribing with a hand-held silicon carbide razor blade while the fiber is under tension. The method is shown in figure 3-14.

Cleaved ends are visually inspected for acceptability with both a 40 power and a 100 power microscope having NA = 0.12 and 0.25. Acceptance is based on a subjective evaluation of smoothness without hackle, lips, breakover or deep notches at the point of scribing, and perpendicularity. Glass chips or foreign material (dirt, jacketing material, etc.) adhering to the end are removed with adhesive tape.

Visual inspection with only one orientation can be deceptive. For this reason, the ends are examined from different angles and under different types of illumination.

The input end is mounted on the x-y-z positioner with the mode stripper in place. The launch spot and the fiber end is viewed for alignment with the vidicon and monitor. The fiber output ends are taped to a flat surface in front of the detector so the axes of the two fibers, if extended, would intersect at the surface of the large area detector. Care is taken to ensure that all the power out of the fiber is collected by the detector.

With the source aperture in place, the appropriate diaphragm set at the launch lens, and the filter wheel set, the positioner is adjusted to place the input face of the fiber at image plane of L_3. Minor axial repositioning to maximize transmitted power is done at each wavelength. When small

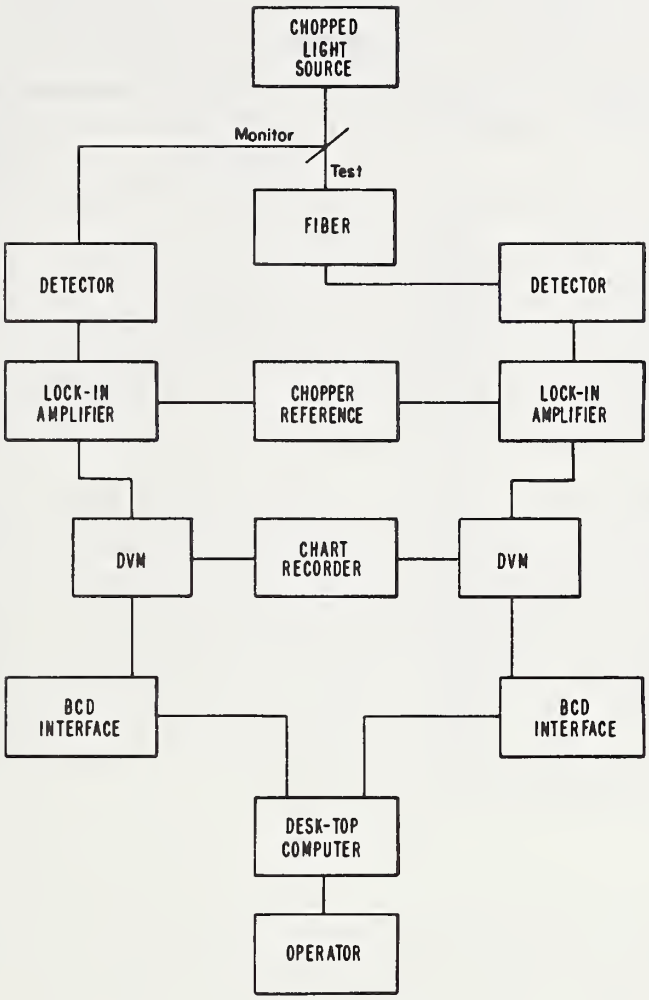

Figure 3-15. Block diagram of measurement configuration.

input spot sizes are used other position criteria may be used. Increasing LNA to improve focusing resolution is sometimes useful.

The lock-in amplifier scale is selected on the basis of expected attenuation and the need to avoid scale change, if possible. The amplifier meter in our case has a decibel scale which can be used to assist in this regard. In so doing, recall that the scale measures electrical power, not volts; thus, 2 dB optical loss will be reflected as 4 dB on the electrical scale.

Figure 3-15 is a block diagram of the configuration. The operator is offered three options in the course of taking data. Each option is offered by a screen prompt followed by a computer pause. The operator must respond before the program will proceed. First, the option of monitoring the light source for drift is offered. Experience has shown that a stabilized power supply eliminates drift, so monitoring the source is not often required. If the source is monitored, a correction for drift is imposed in calculating attenuation. The correction is normally small.

Second, the operator is asked to specify the number of data points taken and the time (in milliseconds) between readings. The selected pause between readings is based on the time constant of the lock-in amplifier. The readings must, of course, be independent, which requires that several time

Table 3.3.

Fiber idenfication	Wavelength (nm)	Method*	Number of measurements	Average attenuation (dB)	Standard deviation (dB)
4103	850	MF	5	2.81	0.05
4103	850	LPS	5	2.75	0.04
4103	1300	MF	3	1.62	0.04
4103	1300	LPS	2	1.65	0.02
5202	850	MF	4	1.98	0.09
5202	850	LPS	3	2.18	0.04
5202	1300	MF	3	1.03	0.01
5202	1300	LPS	3	0.92	0.02
7502	850	MF	5	5.83	0.07
7502	850	LPS	2	5.61	0.01
7502	1300	MF	6	1.85	0.05
7502	1300	LPS	3	1.59	0.01

*MF = mode filter; LPS = limited phase space

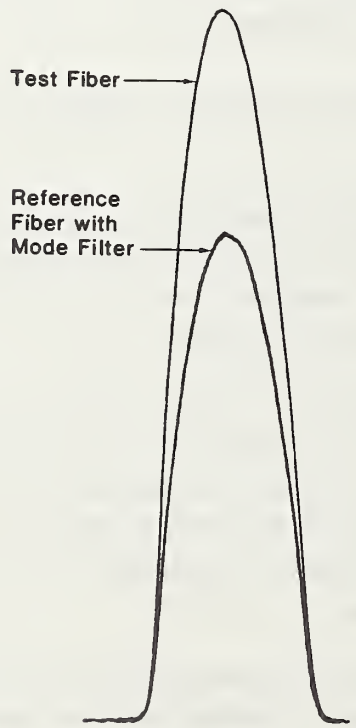

Figure 3-16. Typical far-field pattern of test fiber and reference fiber with mode filter at 850 nm.

constants elapse between readings. It is sometimes true that the signal-to-noise ratio depends on the number of time constants between readings. If so, the selected pause is adjusted accordingly. The average reading and the standard deviation of the readings reach steady state after about 25 readings. Typically, 30 to 50 readings are taken for each measurement. The additional time consumed by taking 50 data points rather than 30 is small and leads to more confidence in the results.

3.8 Some Results

Measurement results are presented here for three telecommunication-grade fibers. Attenuation was measured at 850 nm and 1300 nm. The mode filter was qualified only at 850 nm for each fiber. Figure 3-16 shows the far-field patterns taken for one of the fibers. These plots are typical of those seen by the system being used here. Table 3.3 gives the results of the measurements of the three fibers; the measurement precision is ±0.1 dB.

The data show no clear indication of one launch condition yielding attenuation values consistently lower or higher than the other. The greatest difference encountered is about 0.3 dB on fiber 7502 at 1300 nm. In that case, the mode filter launch yields attenuation that is higher than that found using the LPS launch. Fiber 4103 has nominal length of 0.97 km, fiber 5202 is about 1.1 km long and fiber 7502 is about 2.2 km. The data for fiber 5202 was taken using a mixture of the cut-back and the two-fiber methods. The data show that the standard deviation was not adversely affected in going from one method to the other.

4. Measurement Comparisons and Results

The procedures discussed in this document have evolved over several years; they are based on the desire to define techniques that lead to usable and realistic predictions of attenuation in long fiber links. The procedures described are approved and sanctioned by the EIA (Electronics Industries Association), who drafted them and guided them through the approval stage.

A comprehensive interlaboratory comparison was conducted during 1980 to establish confidence and provide a definitive evaluation of the EIA procedure [23]. In the following, we discuss that interlaboratory test. The material presented here is exerpted from reference 23.

4.1 Participants and Instructions

The participants in the interlaboratory comparison included NBS and nine vendors who are members of the EIA. These included most US and some Canadian manufacturers of fiber or fiber cable. Participants were given a brief description of the physical characteristics (manufacturer's specifications) of the test fibers and special handling instructions. The following instructions were given.

For mode filter launch:

1. Overfill the test fiber in both spot size and numerical aperture, then measure the long fiber far-field radiation pattern and determine θ_1, the full width at the 5 percent intensity points.
2. Apply a mode filter to the test fiber and adjust until the far-field radiation pattern at the 5 percent intensity points from a 1.8 m length is θ_1 with a tolerance of +0, -7 percent (the current tolerance is -3 ± 3 percent). This procedure qualifies the mode filter for the attenuation measurement.

3. Apply the same mode filter to the test fiber, then measure the attenuation (mode filter is in place and undisturbed for both long and short length measurements) using a reference (cutback) length of 1.8 ± 0.1 m and some type of cladding mode stripper.

For LPS launch:

1. Use beam optics to produce a launch spot with a diameter at the 50 percent intensity points of 70 ± 5 percent of the core diameter.
2. The launch numerical aperture determined at the 5 percent intensity points shall be 70 ± 5 percent of the fiber numerical aperture.
3. Use manufacturer's numbers for core size and NA.
4. The launch spot shall be centered on the fiber core.
5. Attenuation shall be measured using a reference length of 1.8 ± 0.1 m and some type of cladding mode stripper.

In addition to a test of the restricted launch conditions, the interlaboratory tests provided an opportunity to compare the results with those obtained using an overfilled launch condition. This provided additional insight into the effect of the two launch conditions on measured attenuation. The participants were asked to measure attenuation using overfill conditions, according to the following instructions.

Overfilled Launch:

1. Use a launch spot size which overfills the fiber core.
2. Use a launch numerical aperture of 0.24 or the next larger size available to you.
3. In making the measurement, use a reference (cutback) length of 1.8 ± 0.1 m and some type of cladding mode stripper.

The test fiber parameters are given in table 4.1.

4.2 Comparison Results

This interlaboratory comparison yielded data on the stability of fibers that are subjected to repeated handling and shipping. The fibers were returned to NBS and remeasured after each participant's measurement, to identify trends. One of the four fibers (fiber B) tended toward decreasing attenuation so it was retired after five participants. The one standard deviation spread for fibers A, B, C, and D was 0.06, 0.10, 0.08, and 0.10 dB/km; precision of the NBS measurement system was typically 0.1 dB/km at 850 nm, the wavelength of interest in this comparison test.

Each participant was told the fiber length and results were reported in dB/km. Participants typically used 10 m of fiber to complete all measurements and were requested to use no more fiber than needed to make two measurements of each quantity. NBS monitored the fiber length so results could be given in dB/km.

Attenuation results from 10 participants are summarized in figures 4-1 through 4-4, table 4.2, and table 4.3. A few reported values were clearly outside the dominant distributions. Of 60 reported

Table 4.1. Nominal properties of comparison fibers

Fiber	Cladding O.D., μm	Core dia., μm	Buffer coating thickness, μm	Numerical aperture	Reel dia., cm	Length, km
A	125	60	170	0.24	26	2
B	125	50	70	0.16	32	2
C	125	60	70	0.18	22	2
D	125	60	thin polymer	0.20	30	0.9

fibers. Average system precision for the ten participants is 0.15 dB/km. One standard deviation measurement spread is 0.24, 0.11, 0.12, and 0.43 dB/km for fibers A, B, C, and D; the average is 0.23 dB/km. Approximately two-thirds of the participants used the mode filter procedure; the remainder chose the LPS method. Mode filters included mandrel wraps, serpentine bends, and a dummy fiber. The average mode filter value minus the average beam optics value is +0.15, -0.02, -0.07, and +0.30 dB/km for fibers A, B, C, and D. In all cases these offsets are less than one standard deviation of the mode filter values by themselves. Therefore, systematic differences between the two approaches are too small to appear in the comparisons with a significant level of confidence. Greater differences between the two techniques might appear in fibers which have high differential mode attenuation. The next section gives measurement results on two fibers which have high differential mode attenuation. These data, supplied by P. Reitz of the Corning Glass Works, indicates little systematic difference between the two techniques (for these fibers) if the mode filter far-field pattern from the reference length is chosen to be in the center of its allowed tolerance. (See additional comments in the following section.)

Overfilled launch results are given in table 4.3 for the four fibers. One standard deviation is 0.39, 0.14, 0.04, and 0.47 dB/km for fibers A, B, C, and D; the average is 0.26 dB/km. Seven participants reported initially aligning the fiber under test for peak transmitted power while two placed the fiber at the center of the launch spot; there is no significant difference between the two alignment methods for overfilled launch conditions. An earlier comparison had a 0.6 dB/km standard deviation [20]. Also, the average of the standard deviations obtained for overfilled launching conditions, 0.26 dB/km, does not differ much from the 0.23 dB/km resulting from the restricted launch.

Participants did significantly better on some fibers than on others. This may be due to differences in the DMA (differential mode attenuation) for the fibers. The smallest measurement spread is for fiber C, which exhibits almost no differential mode attenuation. The difference between overfilled and restricted launch attenuations is a measure of differential mode attenuation in a fiber; differences for the four fibers in ascending order are 0.03, 0.28, 0.42, and 0.80 dB/km for fibers C, B, A, and D, respectively. This same order occurs when fibers are listed according to increasing measurement spread. The attenuation in high DMA fibers is more sensitive to launching conditions.

Fiber D has a high OH^- concentration. The proximity of the 875 nm OH^- absorption line to the 850 nm measurement wavelength may have affected the results. For example, the slope of the spectral attenuation for fiber D at 860 nm is +0.06 dB/nm, whereas when loss is limited by a Rayleigh scattering as in C, the same slope is -0.01 dB/nm. A small positive offset from the measurement wavelength in addition to a broad source linewidth would result in a higher measured attenuation (fig. 4-5) (some participants reported using 20 nm source linewidths).

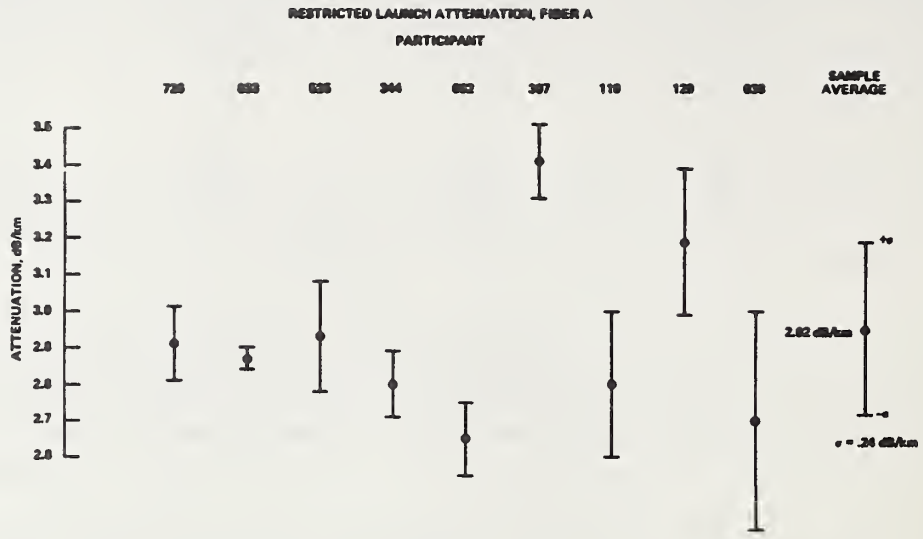

Figure 4-1. Results of restricted launch attenuation measurements, fiber A.

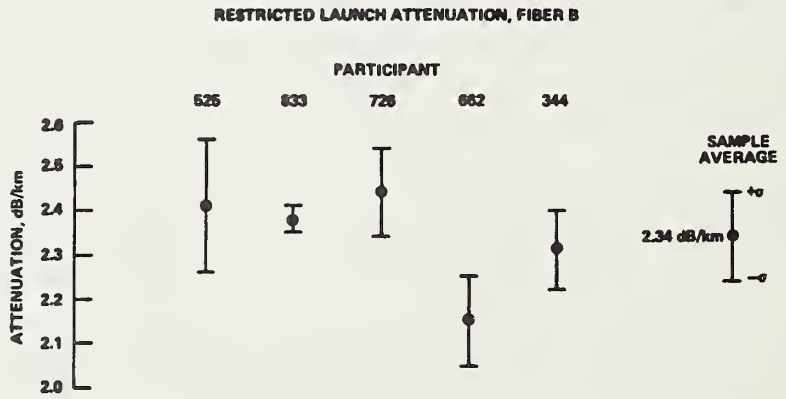

Figure 4-2. Results of restricted launch attenuation measurements, fiber B.

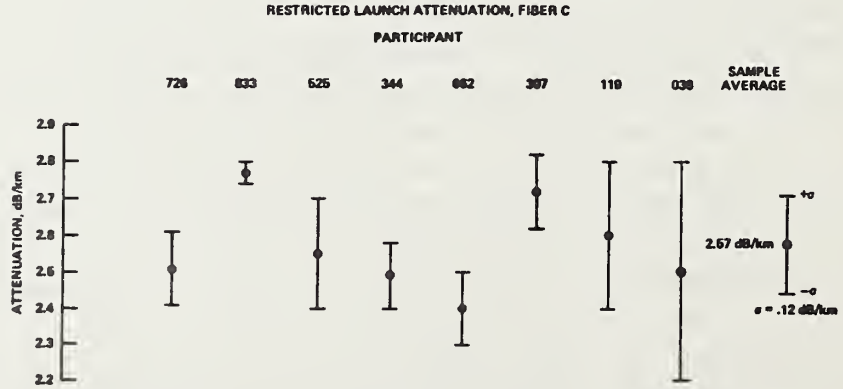

Figure 4-3. Results of restricted launch attenuation measurements, fiber C.

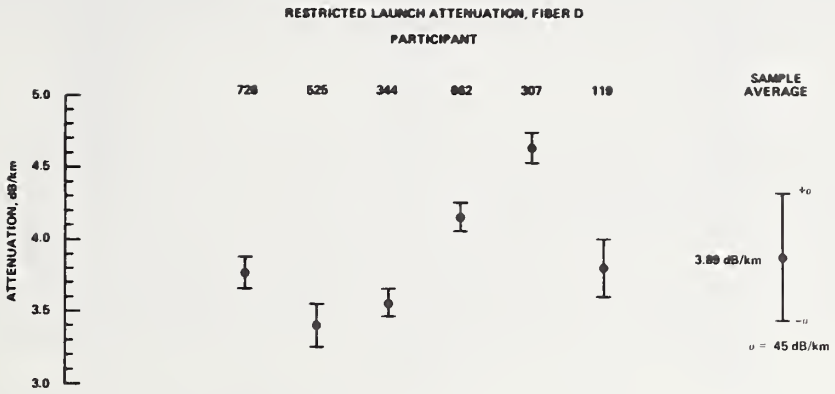

Figure 4-4. Results of restricted launch attenuation measurements, fiber D.

4.3 Attenuation Measurements in High-DMA Fibers

The largest discrepancies between the LPS or beam optics and the mode filter launch conditions occur in fibers having high DMA. This section gives results for two 1-km fibers that have higher DMA than the comparison fibers. For these fibers, attenuation differences between overfilled and restricted launch at 850 nm are 1.74 and 0.72 dB/km. Table 4.4 shows the difference between the LPS and the mode filter launch implemented at the mid-point and extremes of the specified tolerance on the match of far-field radiation patterns. Mode filters are specified from the far-field radiation angle at the 5 percent intensity points. If θ_L is the radiation angle produced using overfilled launching conditions to the test fiber without a mode filter, and θ_S is the radiation angle from the short

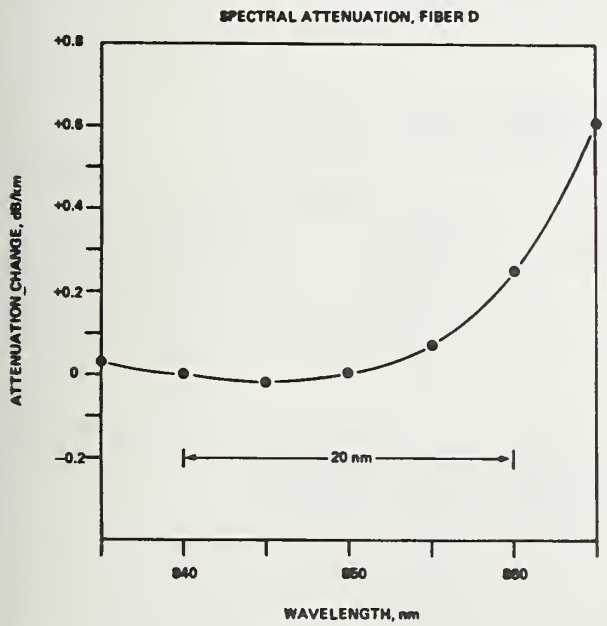

Figure 4-5. Spectral attenuation change with respect to the comparison wavelength of 850 nm for fiber D. An OH^- absorption line occurs at 875 nm.

Table 4.2. Restricted launch attenuation, 850 nm (dB/km)

Participant	Fiber A	Fiber B	Fiber C	Fiber D
726	2.91	2.44	2.51	3.77
833	2.87	2.38	2.77	-
525	2.93	2.41	2.55	3.40
344	2.80	2.31	2.49	3.56
662	2.65	2.15	2.40	4.15
307	3.41	-	2.72	4.6
119	2.8	-	2.6	3.8
129	3.19	-	-	-
038	2.7	-	2.5	-
902	-	-	-	-
Mean	2.92	2.34	2.57	3.89
Standard deviation	0.24	0.12	0.12	0.43

Table 4.3. Overfilled launch attenuation, 850 nm (dB/km)

Participant	Fiber A	Fiber B	Fiber C	Fiber D
726	3.26	2.67	2.60	4.95
833	3.08	2.46	2.63	-
525	3.03	2.78	2.55	4.31
344	3.04	2.55	2.54	4.97
662	-	-	-	-
307	3.38	-	2.60	4.77
119	3.2	-	2.6	5.2
129	3.48	-	-	-
038	3.3	-	2.66	-
902	4.29	-	2.58	3.94
Mean	3.34	2.62	2.60	4.69
Standard deviation	0.39	0.14	0.04	0.47

Table 4.4. Attenuation using mode filter and beam optics launches in two high DMA fibers at wavelengths of 850 and 1300 nm (dB/km)

	Fiber #1		Fiber #2	
	850 nm	1300 nm	850 nm	1300 nm
Overfilled launch	4.16	2.97	3.25	1.74
LPS launch; 70% core, 70% NA	2.42	1.11	2.53	0.94
Attenuation difference	1.74	1.86	0.72	0.80
Mode filter attenuation - 70/70 beam optics attenuation for various values of Δ the fractional far-field radiation angle mismatch parameter				
$\Delta = 0$	+0.16	+0.11	+0.20	+0.38
$\Delta = -3\%$	-0.05	-0.04	+0.03	+0.12
$\Delta = -7\%$	-0.27	-0.29	-0.11	-0.08

(reference) length with the mode filter applied, then $\Delta\theta = (\theta_S - \theta_L)/\theta_L$. For the comparisons, the mode filters had to produce $\Delta\theta$ values between 0 and -7 percent. At both 850 and 1300 nm, the mode filter attenuation values at the tolerance extremes (0 and -7 percent) straddle the LPS values. At -3 percent, near the tolerance mid-point, attenuation values obtained by the two approaches are nearly the same.

The results experienced in these tests may not be typical of the results from other high DMA fibers. This is because the exact nature of DMA may be instrumental to the relationship between the LPS and the mode filter launch. Some fibers may experience high DMA among low order modes but low DMA among high order modes. For other fibers, the converse may be true. For still other fibers, high DMA may prevail only in the mid-range of modes. The results given in table 4.4 are not typical of the results that would obtain under these diverse conditions.

4.4 Summary of Interlaboratory Comparisons

The results described above suggest the following:

1. Measurement agreement for attenuation has improved since the last NBS-sponsored comparisons [24].
2. Uncabled fibers exhibit good stability as comparison fibers if proper attention is given to buffering and winding configuration.
3. Restricted and overfilled launching conditions for attenuation measurements yield similar standard deviations on some types of graded-index fiber.
4. The LPS and mode filter launch conditions yield nearly the same attenuation on many types of long graded-index fibers.
5. The 0.12 and 0.04 dB/km standard deviations obtained for fiber C indicate systematic differences between participants. These arise from various non-modal effects such as failure to strip cladding light, nonlinear detection, and incorrect wavelength. Systematic differences are near or less than the average claimed system precision of 0.15 dB/km. As DMA decreases in future high-quality fibers, measurement agreement is expected to improve.
6. Standard deviations on some fibers are near typical system precisions. Further improvements will require better system precisions or the use of many measurements and confidence intervals.

The authors are indebted to Dr. M. A. Holzman, Mr. A. G. Hanson, Mr. P. R. Reitz, and Dr. A. H. Cherin for constructive comments. The discussion on phase space, in particular, was revised after lengthy discussions with Mel Holzman. His help is sincerely appreciated. Finally, we acknowledge the gracious and expert editorial assistance of Edie DeWeese.

5. References

[1] Olshansky, R.; Blankenship, M. G.; Keck, D. B. Launch-dependent attenuation measurements in graded-index fibers. Second European Conference on Optical Fibre Communication, Paris; 1976.

[2] Vella, P. J.; Abe, K.; Kapron, F. P. Precise measurement of fiber attenuation. Technical Digest, Symposium on Optical Fiber Measurements. Nat. Bur. Stand. (U.S.) Spec. Publ. 641; 1982.

[3] Personick, S. D. Time dispersion in dielectric waveguides. Bell Syst. Tech. J. 50:843; 1971.

[4] Chinnock, E. L.; Cohen, L. G.; Holden, W. S.; Standley, R. D.; Keck, D. B. The length dependence of pulse spreading in the CGW-Bell-10 optical fiber. Proc. IEEE 61:1499; 1973.

[5] Keck, D. B. Spatial and temporal power transfer measurements on a low-loss optical waveguide. Appl. Opt. 15:1882; 1974.

[6] Olshansky, R.; Oaks, S. M. Differential mode attenuation measurements in graded-index fibers. Appl. Opt. 17:1830; 1978.

[7] Olshansky, R.; Oaks, S. M.; Keck, D. B. Measurement of differential mode attenuation in graded-index optical waveguides. Technical Digest, Topical Meeting on Optical Fiber Transmission, Williamsburg; Paper TuE5; 1977.

[8] Arnaud, J. A. Beam and fiber optics (chapt. 4). Academic Press: New York; 1976.

[9] Holmes, G. T. Propagation parameter measurements of optical waveguides. In Fiber Optics for Communications and Control, SPIE Publication 224; 1980.

[10] Gallawa, R. L. On the definition of fiber numerical aperture. Electro-Optical System Design, 46; April 1982.

[11] Hanson, A. G.; Bloom, L. R.; Cherin, A. H.; Day, G. W.; Gallawa, R. L.; Gray, E. M.; Kao, C.; Kapron, F. P.; Kawasaki, B. S.; Reitz, P.; and Young, M. Optical waveguide communications glossary. Nat. Bur. Stand. (U.S.) Handb. 140; 1982.

[12] Cherin, A. H.; Head, E. D.; Lovelace, C. R.; Gardner, W. B. Selection of mandrel wrap mode filters for optical fiber loss measurement. Fiber Integ. Opt. 4:49; 1982.

[13] Agarwal, A. K.; Karstensen, H.; Unrau, U. Modal behavior of various mode mixers and mode filters for optical fiber measurements. Technical Digest, Symposium on Optical Fiber Measurements. Nat. Bur. Stand. (U.S.) Spec. Publ. 641; 1982.

[14] Reitz, P. R. Measuring optical waveguide attenuation: The LPS method. Opt. Spectra, 48; August 1981.

[15] Franzen, D. L.; Day, G. W.; Gallawa, R. L. Standardizing test conditions for characterizing fibers. Laser Focus, 103; August 1981.

[16] Technical Digest, Symposium on Optical Fiber Measurements. Nat. Bur. Stand. (U.S.) Spec. Publ. 597; 1980.

[17] Tokuda, M.; Seikai, S.; Yoshida, K.; Uchida, N. Measurement of baseband frequency response of multimode fibre by using a new type of mode scrambler. Electron. Lett. 13:146; 1977.

[18] Electronics Industries Association. Light launch conditions for long length graded-index optical fiber spectral attenuation measurement. FOTP 50; 1982.

[19] Young, M. Optics and lasers, an engineering physics approach. New York: Springer-Verlag; 1977.

[20] Kim, E. M.; Franzen, D. L. Measurement of far-field and near-field radiation patterns from optical fibers. Nat. Bur. Stand. (U.S.) Tech. Note 1032; 1981.

[21] Sladen, F. M. E.; Payne, D. N.; Adams, M. J. Definitive profile-dispersion data for germanium-doped silica fibres over an extended wavelength range. Electron. Lett. 15:469, 1979.

[22] Mandel, John. The statistical analysis of experimental data. New York: Interscience Publishers; 1964.

[23] Franzen, D. L.; Day, G. W.; Danielson, B. L.; Chamberlain, G. E.; Kim, E. M. Interlaboratory measurement comparison to determine the attenuation and bandwidth of graded-index optical fibers. Appl. Opt. 20:2412; 1981.

[24] Day, G. W.; Chamberlain, G. E. Attenuation measurements of optical fiber waveguides: An interlaboratory comparison among manufacturers. Nat. Bur. Stand. (U.S.) NBSIR 79-1608; 1979.

Appendix A. Mode Volume and Limited Phase Space

This appendix is addressed to the plausibility of agreement in the measured results when using the LPS and the mode-filter launch conditions. The LPS launch depends only on conditions at the input face of the fiber. The mode-filter launch is based on the far-field pattern of the fiber. Nevertheless, the plausibility of agreement is discussed in section 2.3. The subject is pursued further by examining the number of modes excited by a limited phase space launch.

The number of guided modes (M) in a heavily overmoded fiber having a power-law refractive index profile is found by integrating the normalized wave number over the fiber core and multiplying by 2 to account for the two allowed polarization states:

$$M = \frac{2}{4\pi} \int \int [k^2(x,y) - k_2^2)\, dx\, dy. \tag{A-1}$$

Converting to circular cylindrical coordinates and assuming a power-law profile with profile parameter g:

$$k^2 = \left(\frac{2\pi}{\lambda}\right)^2 n_1^2[1 - 2\Delta(r/a)^g], \tag{A-2}$$

$$k_2^2 = \left(\frac{2\pi}{\lambda}\right)^2 n_1^2[1 - 2\Delta], \tag{A-3}$$

where n_1 is the refractive index at r = 0 and

$$n(r) = n_1[1 - 2\Delta(r/a)^g]^{1/2}. \tag{A-4}$$

Consider the mode volume (the number of guided modes) between r = 0 and r = u:

$$M(u) = \left(\frac{2\pi}{\lambda}\right)^2 \frac{2\Delta\, n_1^2}{2\pi} \int_0^{2\pi} \int_0^{u} [1 - (r/a)^g]\, r\, d\phi\, dr. \tag{A-5}$$

Several special cases are of interest ($V = (2\pi a/\lambda)\sqrt{n_1^2 - n_2^2}$):

Case I: u = a, g = ∞ (step index fiber) (A-6)
$M = V^2/2$

Case II: u = a, g = 2 (parabolic profile) (A-7)
$M = V^2/4$

Case III: $u = a/\sqrt{2}$, g = 2 (A-8)
$M = (V^2/4) \cdot 3/4$

Cases I and II are well known; they imply a 3 dB loss when coupling from a step-index fiber to a parabolic profile fiber. Cases II and III are of interest to this discussion. They imply a loss of 1.25 dB in coupling a filled parabolic fiber (filled in both core size and numerical aperture) to an identical fiber through an aperture of radius $a/\sqrt{2}$, using a perfect butt joint.

This 1.25 dB loss is consistent with the concepts of LPS. To see this, note first that leaky modes should be ignored since they were not included in the foregoing. Consider, then, eqs (2-27):

$$\frac{P_{LPS} + P_d}{P_{LPS} + 2P_d} = 3/4 \ (1.25 \text{ dB}), \tag{A-9}$$

Which agrees with eqs (A-8) and (A-7).

NBS-114A (REV. 2-8C)

U.S. DEPT. OF COMM. BIBLIOGRAPHIC DATA SHEET (See instructions)	1. PUBLICATION OR REPORT NO. NBS TN-1060	2. Performing Organ. Report No.	3. Publication Date June 1983

4. TITLE AND SUBTITLE

Measurement of Multimode Optical Fiber Attenuation

5. AUTHOR(S)

R. L. Gallawa, G. E. Chamberlain, G. W. Day, D. L. Franzen, and M. Young

6. PERFORMING ORGANIZATION (If joint or other than NBS, see instructions)

NATIONAL BUREAU OF STANDARDS
DEPARTMENT OF COMMERCE
WASHINGTON, D.C. 20234

7. Contract/Grant No.

8. Type of Report & Period Covered

9. SPONSORING ORGANIZATION NAME AND COMPLETE ADDRESS (Street, City, State, ZIP)

10. SUPPLEMENTARY NOTES

☐ Document describes a computer program; SF-185, FIPS Software Summary, is attached.

11. ABSTRACT (A 200-word or less factual summary of most significant information. If document includes a significant bibliography or literature survey, mention it here)

This document is one of a series which describes optical fiber measurement capabilities at the National Bureau of Standards. We concentrate here on the measurement of attenuation of multimode, telecommunication-grade fibers for the wavelength range of 850 nm to 1300 nm. The document begins by discussing the need for restricted launch conditions, the most fundamental and crucial aspect of precise attenuation measurements. The limited phase space launch (also called the beam optics launch) and the mode filter launch are discussed. Attention then turns to the practical matter of ensuring that the conditions of the restricted launch are met. Discussions of system noise and system linearity are also included. The document describes measurement procedure and results obtained in the laboratory using three typical fibers. Results are presented for the two wavelengths of current interest: 850 nm and 1300 nm. The procedures are applicable to any wavelength, however. The document touches briefly on the matter of monomode fibers. Finally, a summary of the results from an interlaboratory comparison are presented to give perspective to the stability of a fiber subjected to handling and shipping.

12. KEY WORDS (Six to twelve entries; alphabetical order; capitalize only proper names; and separate key words by semicolons)

attenuation; attenuation measurement; fiber measurement; optical fibers; optical waveguides.

13. AVAILABILITY

☒ Unlimited

☐ For Official Distribution. Do Not Release to NTIS

☒ Order From Superintendent of Documents, U.S. Government Printing Office, Washington, D.C. 20402.

☐ Order From National Technical Information Service (NTIS), Springfield, VA. 22161

14. NO. OF PRINTED PAGES

52

15. Price

$4.00

☆U.S. GOVERNMENT PRINTING OFFICE: 1983–679-890/342

USCOMM-DC 6043-P80

NBS TECHNICAL PUBLICATIONS

PERIODICALS

JOURNAL OF RESEARCH—The Journal of Research of the National Bureau of Standards reports NBS research and development in those disciplines of the physical and engineering sciences in which the Bureau is active. These include physics, chemistry, engineering, mathematics, and computer sciences. Papers cover a broad range of subjects, with major emphasis on measurement methodology and the basic technology underlying standardization. Also included from time to time are survey articles on topics closely related to the Bureau's technical and scientific programs. As a special service to subscribers each issue contains complete citations to all recent Bureau publications in both NBS and non-NBS media. Issued six times a year. Annual subscription: domestic $18; foreign $22.50. Single copy, $4.25 domestic; $5.35 foreign.

NONPERIODICALS

Monographs—Major contributions to the technical literature on various subjects related to the Bureau's scientific and technical activities.

Handbooks—Recommended codes of engineering and industrial practice (including safety codes) developed in cooperation with interested industries, professional organizations, and regulatory bodies.

Special Publications—Include proceedings of conferences sponsored by NBS, NBS annual reports, and other special publications appropriate to this grouping such as wall charts, pocket cards, and bibliographies.

Applied Mathematics Series—Mathematical tables, manuals, and studies of special interest to physicists, engineers, chemists, biologists, mathematicians, computer programmers, and others engaged in scientific and technical work.

National Standard Reference Data Series—Provides quantitative data on the physical and chemical properties of materials, compiled from the world's literature and critically evaluated. Developed under a worldwide program coordinated by NBS under the authority of the National Standard Data Act (Public Law 90-396).

NOTE: The principal publication outlet for the foregoing data is the Journal of Physical and Chemical Reference Data (JPCRD) published quarterly for NBS by the American Chemical Society (ACS) and the American Institute of Physics (AIP). Subscriptions, reprints, and supplements available from ACS, 1155 Sixteenth St., NW, Washington, DC 20056.

Building Science Series—Disseminates technical information developed at the Bureau on building materials, components, systems, and whole structures. The series presents research results, test methods, and performance criteria related to the structural and environmental functions and the durability and safety characteristics of building elements and systems.

Technical Notes—Studies or reports which are complete in themselves but restrictive in their treatment of a subject. Analogous to monographs but not so comprehensive in scope or definitive in treatment of the subject area. Often serve as a vehicle for final reports of work performed at NBS under the sponsorship of other government agencies.

Voluntary Product Standards—Developed under procedures published by the Department of Commerce in Part 10, Title 15, of the Code of Federal Regulations. The standards establish nationally recognized requirements for products, and provide all concerned interests with a basis for common understanding of the characteristics of the products. NBS administers this program as a supplement to the activities of the private sector standardizing organizations.

Consumer Information Series—Practical information, based on NBS research and experience, covering areas of interest to the consumer. Easily understandable language and illustrations provide useful background knowledge for shopping in today's technological marketplace.

Order the **above** *NBS publications from: Superintendent of Documents, Government Printing Office, Washington, DC 20402.*

Order the **following** *NBS publications—FIPS and NBSIR's—from the National Technical Information Services, Springfield, VA 22161.*

Federal Information Processing Standards Publications (FIPS PUB)—Publications in this series collectively constitute the Federal Information Processing Standards Register. The Register serves as the official source of information in the Federal Government regarding standards issued by NBS pursuant to the Federal Property and Administrative Services Act of 1949 as amended, Public Law 89-306 (79 Stat. 1127), and as implemented by Executive Order 11717 (38 FR 12315, dated May 11, 1973) and Part 6 of Title 15 CFR (Code of Federal Regulations).

NBS Interagency Reports (NBSIR)—A special series of interim or final reports on work performed by NBS for outside sponsors (both government and non-government). In general, initial distribution is handled by the sponsor; public distribution is by the National Technical Information Services, Springfield, VA 22161, in paper copy or microfiche form.

U.S. Department of Commerce
National Bureau of Standards

Washington, D.C. 20234
Official Business
Penalty for Private Use $300

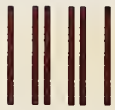

POSTAGE AND FEES PAID
U.S. DEPARTMENT OF COMMERCE
COM-215

THIRD CLASS
BULK RATE